

CELLULARITY FOR WEIGHTED KLRW ALGEBRAS OF TYPES B , $A^{(2)}$, $D^{(2)}$

ANDREW MATHAS AND DANIEL TUBBENHAUER

ABSTRACT. This paper constructs homogeneous affine sandwich cellular bases of weighted KLRW algebras in types $B_{\mathbb{Z}_{\geq 0}}$, $A_{2,e}^{(2)}$, $D_{e+1}^{(2)}$. Our construction immediately gives homogeneous sandwich cellular bases for the finite dimensional quotients of these algebras. Since weighted KLRW algebras generalize KLR algebras, we also obtain bases and cellularity results for the (finite dimensional) KLR algebras.

CONTENTS

1. Introduction	1
2. Sandwich cellular algebras	2
3. Reminders about weighted KLRW algebras	3
4. The strategy	7
5. The bases	9
6. Proof of cellularity	19
References	22

1. INTRODUCTION

KLR algebras, or quiver Hecke algebras, are certain graded infinite dimensional algebras attached to a quiver. These algebras arose in categorification and categorical representation theory, see e.g. [KL09], [KL11], [Rou08] or [Rou12]. They admit finite dimensional quotients, called *cyclotomic KLR algebras*. Both, KLR algebras and their cyclotomic quotients, play crucial roles in modern representation theory and have attracted a lot of attention since their introduction.

A crucial problem is to determine whether these algebras are (graded) cellular in the sense of [GL96], or some variation of cellularity such as affine cellular [KX12]. It turns out that they tend to be graded affine cellular in the infinite dimensional case, see e.g. [KL15], and graded cellular in the finite dimensional case, see e.g. [HM10]. Even better, in both cases one can write down explicit homogeneous (affine) cellular bases. However, to the best of our knowledge and modulo weighted KLRW algebras, there is no clear relationship between the bases for the infinite dimensional algebras and the bases for their finite dimensional quotients.

Weighted KLRW algebras are generalizations of KLR algebras that were introduced by Webster. See, for example, [Web19], [Web17], [Bow17] or [MT21]. Similar to KLR algebras, these algebra also admit finite dimensional quotients. With appropriate choices, the KLR algebras are idempotent subalgebras of the weighted KLRW algebras. This, for example, means that there is no immediate relationship between the simple modules of weighted KLRW and KLR algebras, and care must be taken when comparing these algebras.

In the **AC types**, that is, types $A_{\mathbb{Z}}$, $A_e^{(1)}$, $C_{\mathbb{Z}_{>0}}$, $C_e^{(1)}$, we showed [MT21] that one of the key properties of these weighted KLRW algebras is that in the they have homogeneous affine cellular bases constructed in the style of low dimensional topology, and these bases automatically descend to the finite dimensional quotients. As a result, we obtained homogeneous (affine) cellular bases for the corresponding KLR algebras and their finite dimensional quotients. Even better, all of these bases work over any commutative integral domain R (for example $R = \mathbb{Z}$).

It is natural to ask whether these constructions can be extended to other types. In this paper we answer this question affirmatively for types $B_{\mathbb{Z}_{\geq 0}}$, $A_{2,e}^{(2)}$, $D_{e+1}^{(2)}$: the **BAD types**. That is, we construct homogeneous affine sandwich cellular bases for weighted KLRW algebras that descend to the finite dimensional quotients. Again, we obtain bases for the corresponding KLR algebras. The sandwich part of our bases corresponding to the finite dimensional quotients is given by copies of the dual numbers $R[X]/(X^2)$, which explains the powers of 2 appearing in the dimension formulas of the finite dimensional KLR algebras. For completeness, we note that the weighted KLRW algebras and their finite dimensional quotients of **BAD types** are actually (affine) cellular; see Remark 2A.7 for a more precise statement. As a consequence we obtain the usual results such as a construction of the graded simple modules and that the decomposition matrix is unitriangular.

Mathematics Subject Classification 2020. Primary: 16G99, 20C08; Secondary: 20C30, 20G43.

Keywords. KLR algebras, diagram algebras, cellular bases, Hecke and Schur algebras.

This paper is a sequel to [MT21], so we assume some familiarity to the definitions and results of that paper. In sequels to this paper we hope to discuss weighted KLRW algebras of other types and their simple modules.

Remark 1.1. The colors used in this paper are not essential and all strings are distinguishable by their thickness and if they are solid or dashed.

Acknowledgments. Want to thank Chris Bowman for a helpful zoom discussion that made us realize several questions related to (affine) sandwich cellular algebras.

Both authors were supported, in part, by the Australian Research Council. In these COVID-19 infested times, we thank the first author's office for sponsoring us for the one hour where the main bulk of the mathematics in this paper was discovered.

2. SANDWICH CELLULAR ALGEBRAS

Cellular algebras were introduced by Graham–Lehrer [GL96]. Over the years many generalizations were discovered. For example, incorporating a grading [HM10], sandwiching a polynomial ring [KX12] or sandwiching any (potentially noncommutative) algebra [GW15], [TV21]. In order, these variations are called *graded cellular*, *affine cellular* and *sandwich cellular* algebras.

Remark 2A.1. Strictly speaking [KX12] sandwich a polynomial ring or a quotient of a polynomial ring. In particular, as we will see, for weighted KLRW algebras of *BAD* types we only need affine cellularity. However, we want to reserve the notion affine for the case of honest polynomial rings, so we tend to say sandwich cellular instead.

The following is a slight reformulation of [MT21, Definition 6B.5], see also [TV21, Section 2].

Definition 2A.2. Let R be a commutative ring with a unit. Let A be a locally unital graded R -algebra. A *graded sandwich cell datum* for A is a quintuple $(\mathcal{P}, T, S, C, \deg)$, where:

- $\mathcal{P} = (\mathcal{P}, \leq)$ is a poset (the *middle set*),
- $T = \bigcup_{\lambda \in \mathcal{P}} T(\lambda)$ is a collection of finite sets (the *bottom/top sets*),
- $S = \bigoplus_{\lambda \in \mathcal{P}} S_\lambda$ is a direct sum of graded algebras S_λ (the *sandwiched algebras*) such that B_λ is a homogeneous basis of S_λ (we write \deg for the degree function on S_λ),
- $C : \prod_{\lambda \in \mathcal{P}} T(\lambda) \times B_\lambda \times T(\lambda) \rightarrow A; (S, b, T) \mapsto C_{ST}^b$ is an injective map (the *basis*),
- $\deg : \prod_{\lambda \in \mathcal{P}} T(\lambda) \rightarrow \mathbb{Z}$ is a function (the *degree*),

such that:

(AC₁) For $b \in B_\lambda$, $S, T \in T(\lambda)$ and $b \in B_\lambda$, $\lambda \in \mathcal{P}$ the element C_{ST}^b is homogeneous of degree $\deg(S) + \deg(b) + \deg(T)$.

(AC₂) The set $\{C_{ST}^b \mid \lambda \in \mathcal{P}, S, T \in T(\lambda), b \in B_\lambda\}$ is a basis of A .

(AC₃) For all $x \in A$ there exist scalars $r_{SU} \in R$ that do not depend on T or on b , such that

$$xC_{ST}^b \equiv \sum_{U \in T(\lambda)} r_{SU} C_{UT}^b \pmod{A^{>\lambda}},$$

where $A^{>\lambda}$ is the R -submodule of A spanned by $\{C_{UV}^c \mid \mu \in \mathcal{P}, \mu > \lambda, U, V \in T(\mu), c \in B_\mu\}$.

(AC₄) Let $A(\lambda) = A^{\geq \lambda}/A^{>\lambda}$, where $A^{\geq \lambda}$ is the R -submodule of A spanned by $\{C_{UV}^c \mid \mu \in \mathcal{P}, \mu \geq \lambda, U, V \in T(\mu), c \in B_\mu\}$. Then $A(\lambda)$ is isomorphic to $\Delta(\lambda) \otimes_{S_\lambda} \nabla(\lambda)$ for free graded right and left S_λ -modules $\Delta(\lambda)$ and $\nabla(\lambda)$, respectively.

The algebra A is a graded *sandwich cellular algebra* if it has a graded sandwich cell datum.

Assume that there is an antiinvolution $(-)^* : A \rightarrow A$ such that:

(AC₅) We have $(C_{ST}^b)^* \equiv C_{TS}^b \pmod{A^{>\lambda}}$.

In this case we call $(\mathcal{P}, T, V, C, \deg, (-)^*)$ *involutive*.

Remark 2A.3. The picture for elements in $\{C_{ST}^b \mid \lambda \in \mathcal{P}, S, T \in T(\lambda), b \in B_\lambda\}$ is:

$$C_{ST}^s \rightsquigarrow \begin{array}{c} \text{---} \\ \text{---} \\ \text{---} \\ \text{---} \\ \text{---} \\ \text{---} \end{array} \begin{array}{c} S \\ b \\ T \end{array}, \quad \begin{array}{c} \text{---} \\ \text{---} \\ \text{---} \\ \text{---} \\ \text{---} \\ \text{---} \end{array} \begin{array}{c} S \\ b \\ T \end{array} \begin{array}{l} \text{top part } S \in T(\lambda), \\ \text{the middle } b \in B_\lambda, \\ \text{bottom part } T \in T(\lambda). \end{array}$$

Note however that, in general, we do not have do we have such a factorization. So this pictures has to be interpreted with care.

We use the following terminology for special cases:

- (a) A graded **affine sandwich cell datum** for A is a graded sandwich cell datum such that, for all $\lambda \in \mathcal{P}$ and for some $n(\lambda) \in \mathbb{Z}_{\geq 0}$, we have $S_\lambda \cong R[X_1, \dots, X_{n(\lambda)}]$.
- (b) A graded **cell datum** for A is a graded sandwich cell datum such that $S_\lambda \cong S$ for all $\lambda \in \mathcal{P}$.

The image of C in A is an **homogeneous sandwich cellular basis** for A . Similarly, we refer to affine sandwich cellular bases etc.

The following **Clifford–Munn–Ponizovskii theorem** parametrizes the simple modules of these types of algebras. To state this result we need some notion.

For each $\lambda \in \mathcal{P}$ there exists a cell module $\Delta(\lambda)$ and a cellular pairing ϕ^λ on $\Delta(\lambda)$, see [TV21, Section 2B]. The pairing ϕ^λ is a symmetric bilinear form. Let $\mathcal{P}^{\neq 0} \subset \mathcal{P}$ be the subset of those λ for which ϕ^λ is nonzero. The illustration to keep in mind is (stolen from [TV21, Section 2B]), the details can be copied from [KX12, Section 2.2]:

$$\phi^\lambda \left(\begin{array}{c} a \\ U \\ b \end{array}, \begin{array}{c} b' \\ D' \end{array} \right) \rightsquigarrow \begin{array}{c} b' \\ D' \\ a \\ U \\ b \end{array} \leftarrow \phi^\lambda \left(\begin{array}{c} U \\ b \end{array}, \begin{array}{c} b' \\ D' \\ a \end{array} \right).$$

Theorem 2A.4. *Let R be a field, and let A be a graded sandwich cellular algebra.*

- (a) *All (graded) simple A -modules are uniquely associated to a $\lambda \in \mathcal{P}^{\neq 0}$, called their **apex**.*
- (b) *Assume that S_λ is unital Artinian or commutative. For a fixed apex $\lambda \in \mathcal{P}^{\neq 0}$ there exists a 1:1-correspondence*

$$\{\text{simple } A\text{-modules with apex } \lambda\} / \cong \xleftrightarrow{1:1} \{\text{simple } S_\lambda\text{-modules}\} / \cong.$$

- (c) *Assume that S_λ is unital graded Artinian or commutative. For a fixed apex $\lambda \in \mathcal{P}^{\neq 0}$ there exists a 1:1-correspondence*

$$\{\text{graded simple } A\text{-modules with apex } \lambda\} / \cong \xleftrightarrow{1:1} \{\text{graded simple } S_\lambda\text{-modules}\} / \cong.$$

Even for non-commutative S_λ the assumption of being unital (graded) Artinian can be avoided under certain conditions, see [TV21, Section 2C] for details.

Proof. The proof is not much different from the general theory as in [GL96], [KX12], [AST18], [ET21], [GW15] or [TV21]. In particular the above is just a (graded) reformulation of [GW15, Theorem 3] and [TV21, Section 2C]. Details are omitted. \square

Remark 2A.5. The bijection in [Theorem 2A.4](#) can be made explicit: the simple A -modules for apex $\lambda \in \mathcal{P}^{\neq 0}$ can be constructed as the simple heads of the cell modules.

Remark 2A.6. The formulation of [Theorem 2A.4](#) is strongly inspired by Green's theory of cells (Green's relations) [Gre51], and the Clifford–Munn–Ponizovskii theorem of semigroup theory, see e.g. [GMS09] for a modern formulation.

Remark 2A.7. If A is involutive and all sandwiched algebras have an (affine sandwich) cellular datum compatible with the sandwich structure on A , then A also has a cell datum that can be constructed by refining the sandwich cell datum on A in an appropriate sense. However, refining the datum can make the natural sandwich datum cumbersome with very little gain. In our case all algebras have (copies of) polynomial rings and dual numbers sandwiched, and both are affine sandwich cellular algebras, and all of our algebras have a refined (affine sandwich) cell datum. Since these are easy algebras, refining the sandwich cell datum for the weighted KLRW algebras as in this paper appears to be unnecessary.

Notation 2A.8. From now on all of our algebras are assumed to be involutive, and we will omit the use of this word. We have separated the involutive condition (AC₅) in [Definition 2A.2](#) from the other axioms because being involutive is not necessary for [Theorem 2A.4](#) to hold.

3. REMINDERS ABOUT WEIGHTED KLRW ALGEBRAS

We recall the basic constructions and statements regarding weighted KLRW algebras. As we assume some familiarity with [MT21], we will be brief.

Notation 3.1. The following conventions used throughout the paper.

- (a) We work over a commutative integral domain R , the ground ring.
- (b) Graded algebra or module will always mean a \mathbb{Z} -graded algebra or module.

- (c) We use the same diagrammatic conventions as in [MT21]:

$$E \circ D = \begin{array}{|c|} \hline E \\ \hline D \\ \hline \end{array}.$$

In particular, left actions and left modules are given by acting from the top. Modules will always be left modules.

3A. Weighted KLRW algebras in a nutshell. The *weighted KLRW algebras* are diagram algebras consisting of *weighted KLRW diagrams* (diagrams for short). These diagrams have three types of strings: *solid*, *ghost* and *red strings*. All of these strings are labeled, and we will illustrate these as

$$\text{solid} : \begin{array}{|c|} \hline \\ \hline \\ \hline \end{array}, \quad \text{ghost} : \begin{array}{|c|} \hline i \\ \hline \\ \hline \end{array}, \quad \text{red} : \begin{array}{|c|} \hline \\ \hline i \\ \hline \end{array},$$

where the label under the solid and red strings and over the ghost strings. The labels on the strings are also called *residues*.

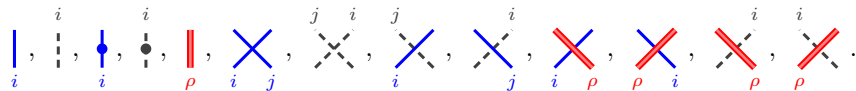
The weighted KLRW algebras depend on the following input:

- (a) An oriented quiver $\Gamma = (I, E)$ with countable vertex set I and countable edge set E arising from a symmetrizable generalized Cartan matrix. Hereby we choose an orientation on the simply laced edges. (The choice of orientation does not play an essential role, cf. [MT21, Proposition 3A.1].) We let $e + 1 = \#I$ be the number of vertices, allowing $e = \infty$. The most important edges for this paper are single and double edges, written as $i \rightarrow j$ respectively $i \Rightarrow j$, and these are the edges relevant for the quivers in (5A.4). If the multiplicity does not play a role, then we write $i \rightsquigarrow j$ if there is an edge from i to j .
- (b) Let u and v be indeterminates over R . For $i, j \in I$ define *Q -polynomials*

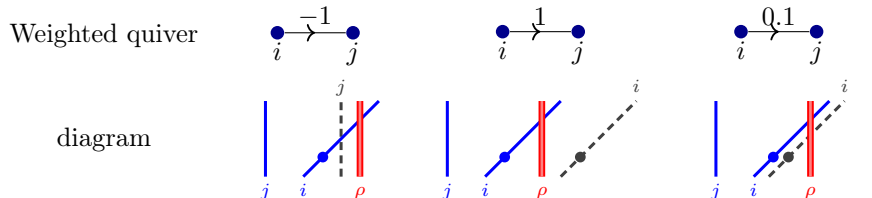
$$(3A.1) \quad Q_{ij}(u, v) = \begin{cases} u - v & \text{if } i \rightarrow j, \\ u - v^2 & \text{if } i \Rightarrow j, \\ 0 & \text{if } i = j, \end{cases} \quad \begin{cases} v - u & \text{if } i \leftarrow j, \\ v - u^2 & \text{if } i \Leftarrow j, \\ 1 & \text{otherwise.} \end{cases}$$

These are Q -polynomials as in [Rou08, Section 3.2.3], [Rou12] or [Web19, Section 2.1]. Recall also that $Q_{i,j,i}(u, v, w) = \frac{Q_{ij}(u,v) - Q_{ij}(u,w)}{w-v}$.

- (c) Non-negative integers $n, \ell \in \mathbb{Z}_{\geq 0}$ and a tuple $\boldsymbol{\rho} = (\rho_1, \dots, \rho_\ell) \in I^\ell$. These are the number of solid strings, the number of red strings (called the *level*) and the red labels, respectively.
- (d) Various types of data determining the positions of the strings. That is, a *solid positioning* $\mathbf{x} = (x_1, \dots, x_n) \in \mathbb{R}^n$, a *ghost shift* $\boldsymbol{\sigma} = (\sigma_\epsilon \in \mathbb{R}_{\neq 0})_{\epsilon \in E}$ which is a weighting of Γ , a *charge* $\boldsymbol{\kappa} = (\kappa_1, \dots, \kappa_\ell) \in \mathbb{R}^\ell$ such that $\kappa_1 < \dots < \kappa_\ell$. The \mathbf{x} , $\boldsymbol{\sigma}$ and $\boldsymbol{\kappa}$ are used to determine the boundary points of solid, ghost and red strings in the diagrams, and are such that there are no overlapping strings.
- (e) A set X of *loadings*, i.e. endpoints for the various strings. We stress that the rank of the weighted KLRW algebras strongly depends on the choice of X .
- (f) Diagrams associated to the data above. These consist of n solid strings labeled by $i \in I$, of ghost strings (explained in the next bullet point), and ℓ red strings labeled by $\boldsymbol{\rho}$. Solid and ghost strings can be additionally decorated with dots. These diagrams are such that their internal points have local neighborhoods of the form



- (g) The ghost strings are determined as follows. For each vertex $i \in I$ and each edge $\epsilon: i \rightsquigarrow j$ and $\sigma_\epsilon > 0$, all solid i -strings get a ghost i -string mimicking the movement of the solid i -strings, having the same dots at the same spots and shifted σ_ϵ units. Similarly for $\sigma_\epsilon < 0$, but then the solid j -strings get ghosts shifted $-\sigma_\epsilon$ units. For example,



(h) There is a degree function on these diagrams given by the local rules

$$\begin{aligned} \deg \begin{array}{c} \bullet \\ | \\ i \end{array} &= 2d_i, & \deg \begin{array}{c} i \\ \bullet \\ | \\ i \end{array} &= 0, & \deg \begin{array}{c} \times \\ / \backslash \\ i \quad j \end{array} &= -\delta_{i,j} 2d_i, & \deg \begin{array}{c} i \\ \times \\ / \backslash \\ j \quad i \end{array} &= \deg \begin{array}{c} i \\ \times \\ / \backslash \\ j \quad i \end{array} = \begin{cases} \langle \alpha_i, \alpha_j \rangle & \text{if } i \rightsquigarrow j, \\ 0 & \text{else,} \end{cases} \\ \deg \begin{array}{c} j \quad i \\ \times \\ / \backslash \\ i \quad j \end{array} &= 0, & \deg \begin{array}{c} \times \\ / \backslash \\ i \quad j \end{array} &= \deg \begin{array}{c} \times \\ / \backslash \\ j \quad i \end{array} = \frac{1}{2} \delta_{i,j} \langle \alpha_i, \alpha_i \rangle, & \deg \begin{array}{c} i \\ \times \\ / \backslash \\ j \quad j \end{array} &= \deg \begin{array}{c} i \\ \times \\ / \backslash \\ j \quad j \end{array} = 0. \end{aligned}$$

Here, $\langle -, - \rangle$ is the Cartan pairing associated to Γ , and (d_0, \dots, d_e) is the symmetrizer.

The **weighted KLRW algebra** $\mathscr{W}_n^P(X)$ is the graded unital associative R -algebra generated by such diagrams with multiplication given by stacking the diagrams and subject to the bilocal relations listed below. Recall that **bilocal** means that one needs to simultaneously apply the relations in local neighborhoods around the solid strings and in the corresponding local neighborhoods around the ghost strings.

(a) The **dot sliding relation** holds, that is, solid and ghost dots can pass through any crossing except:

$$(3A.2) \quad \begin{array}{c} \times \\ / \backslash \\ i \quad i \end{array} - \begin{array}{c} \times \\ / \backslash \\ i \quad i \end{array} = \begin{array}{c} | \\ | \\ i \quad i \end{array} = \begin{array}{c} \times \\ / \backslash \\ i \quad i \end{array} - \begin{array}{c} \times \\ / \backslash \\ i \quad i \end{array}.$$

(b) The **Reidemeister II relation** holds except in the following cases:

$$(3A.3) \quad \begin{array}{c} \times \\ / \backslash \\ i \quad i \end{array} = 0, \quad \begin{array}{c} i \\ \times \\ / \backslash \\ j \quad i \end{array} = Q_{ij}(\mathbf{y}) \begin{array}{c} i \\ | \\ j \end{array} \begin{array}{c} | \\ | \\ j \end{array} \text{ or } \begin{array}{c} i \\ \times \\ / \backslash \\ j \quad i \end{array} = Q_{ji}(\mathbf{y}) \begin{array}{c} | \\ | \\ j \end{array} \begin{array}{c} i \\ | \\ j \end{array} \text{ if } i \rightsquigarrow j, \\ \begin{array}{c} \times \\ / \backslash \\ i \quad i \end{array} = \begin{array}{c} | \\ | \\ i \quad i \end{array}, \quad \begin{array}{c} \times \\ / \backslash \\ i \quad i \end{array} = \begin{array}{c} | \\ | \\ i \quad i \end{array}.$$

(c) The **Reidemeister III relation** holds except in the following cases:

$$(3A.4) \quad \begin{array}{c} i \quad i \\ \times \\ / \backslash \\ j \quad j \end{array} = \begin{array}{c} i \quad i \\ \times \\ / \backslash \\ j \quad j \end{array} - Q_{i,j,i}(\mathbf{y}) \begin{array}{c} i \\ | \\ j \end{array} \begin{array}{c} i \\ | \\ j \end{array} \text{ or } \begin{array}{c} i \\ \times \\ / \backslash \\ j \quad j \end{array} = \begin{array}{c} i \\ \times \\ / \backslash \\ j \quad j \end{array} + Q_{i,j,i}(\mathbf{y}) \begin{array}{c} | \\ | \\ j \end{array} \begin{array}{c} i \\ | \\ j \end{array} \text{ if } i \rightsquigarrow j, \\ \begin{array}{c} \times \\ / \backslash \\ i \quad i \end{array} = \begin{array}{c} \times \\ / \backslash \\ i \quad i \end{array} - \begin{array}{c} | \\ | \\ i \quad i \end{array}.$$

Multiplying by a Q -polynomial adds dots to the corresponding strings. This is explained in more detail in [Notation 3C.2](#) below.

Remark 3A.5. Assume that a vertex $i \in I$ has multiple outgoing edges. Then there are many ghost i -strings, for example

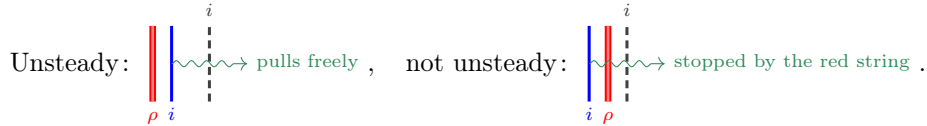
$$\begin{array}{c} \bullet \quad \bullet \quad \bullet \\ \leftarrow 0.75 \quad \rightarrow 1.25 \\ 0 \quad 1 \quad 2 \end{array} \rightsquigarrow \begin{array}{c} | \\ | \\ 1 \end{array} \begin{array}{c} 1 \\ | \\ 1 \end{array}.$$

Note that these two ghost strings are different strings that behave differently because the relations above depend on the edges and not on the residues. In the example above the two ghost 1-strings play different roles. For example, one of them has nontrivial Reidemeister II relations with the 0-strings and the other has nontrivial Reidemeister II relations with the 2-strings.

Remark 3A.6. Note that [\[MT21\]](#) mostly works with $\mathscr{W}_\beta^P(X)$ for β fixing the labels for the solid strings. The difference is not important since $\mathscr{W}_n^P(X) = \bigoplus_{\beta \in Q_n^+} \mathscr{W}_\beta^P(X)$ with Q_n^+ corresponding to the set of all possible labels of the n solid strings.

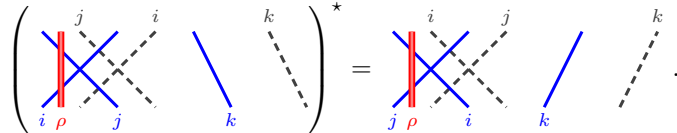
Finally, the **cyclotomic weighted KLRW algebra** $\mathscr{R}_n^P(X)$ is the finite dimensional quotient of $\mathscr{W}_n^P(X)$ by the two-sided ideal generated by all diagrams that factor through an unsteady diagram. A diagram is

unsteady if it contains a solid string that can be pulled arbitrarily far to the right when the red strings are bounded by X . For example, we have



Note that the ghost string mimics its parent solid string, so the solid i -string in the left diagram does indeed pull freely to the right.

3B. Duality and partners. We use the usual *diagrammatic antiinvolution* $(-)^*$ given by (the R -linear extension of) flipping diagrams on their heads. This antiinvolution is the one we use for the homogeneous (affine) sandwich cellular basis. An illustration of the diagrammatic antiinvolution is:

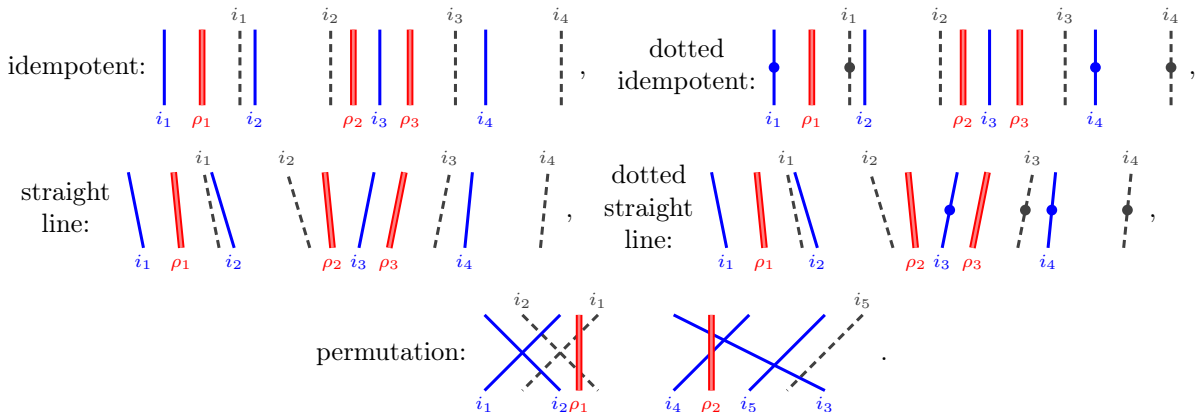


There is a different kind of duality on diagrams, which exists because the relations (3A.2)–(3A.4) come in mirrored pairs. This could mean that they are horizontal mirrors or are obtained by changing the roles of solid and ghost strings, both potentially up to scalars. Most of the relations we will use have this type of duality, and we will only illustrate one of them and call the others *partner relations*. (Note that the partner relations can have different scalars, however this will not play a role for us.)

3C. Some diagrams that we need. We need certain types of diagrams:

- (a) *Idempotent diagrams* are diagrams with no dots and no crossings, and fixed x -coordinates for each strings.
- (b) *Straight line diagrams* which are diagrams with no dots and no crossings.
- (c) Dotted versions of these. That is, *dotted idempotent diagrams* and *dotted straight line diagrams* are dotted diagrams of the respective type.
- (d) *Permutation diagrams* are diagrams with no dots associated (in the evident way) to a reduced expression of a permutation; see [MT21, Definition 3B.1].

Example 3C.1. Examples of these types of diagrams are:



These illustrate (dotted) idempotents, (dotted) straight line and permutation diagrams. \diamond

Notation 3C.2. Let $\mathbf{1}_{\mathbf{x}, \mathbf{i}}$ be the idempotent diagram with bottom boundary given by (\mathbf{x}, \mathbf{i}) , for $\mathbf{x} \in X$ and $\mathbf{i} \in I^n$. We use the notation $p\mathbf{1}_{\mathbf{x}, \mathbf{i}}$, where $p \in R[y_1, \dots, y_n]$ is a polynomial in the indeterminates y_1, \dots, y_n to put dots on $\mathbf{1}_{\mathbf{x}, \mathbf{i}}$ so that y_k corresponds to a dot on the k th solid string.

Additionally, let $\mathfrak{S}_n = \langle s_1, \dots, s_{n-1} \rangle$ be the symmetric group on $\{1, \dots, n\}$ with $s_i = (i, i+1)$. For all $w \in \mathfrak{S}_n$ fix a reduced expression and let $D(w)$ be the associated permutation diagram. As is usual in the KLR world, the diagram $D(w)$ is only well-defined up to some care that needs to be taken, see [MT21, Definition 3B.1] for details.

Finally, as in any idempotent algebra, we only need to (and will) indicate the idempotent diagrams once in any expression.

Example 3C.3. In pictures:

$$\mathbf{1}_{(0,0.5),(i,j)} = \begin{array}{c} i \quad j \\ | \quad | \\ | \quad | \\ i \quad j \end{array}, \quad y_2 \mathbf{1}_{(0,0.5),(i,j)} = \begin{array}{c} i \quad j \\ | \quad | \\ | \quad | \\ i \quad j \end{array}, \quad D(s_1) \mathbf{1}_{(0,0.5),(i,j)} = \begin{array}{c} j \quad i \\ / \quad \backslash \\ \backslash \quad / \\ i \quad j \end{array}.$$

Here we have not drawn red strings. ◇

Definition 3C.4. A diagram D *factors through* S if $D = D'SD''$, for some $D', D'' \in \mathscr{W}_n^\rho(X)$.

Given a straight line diagram S and some $0 < \varepsilon \ll 1$, then there exists an idempotent diagram $L(S)$, called the *left justification* of S , such that S factors through $L(S)$, and $L(S)$ has its strings as far to the left as possible while its coordinates are within the interval defined by X and strings are at least ε apart. (The $\varepsilon > 0$ is only needed to make $L(S)$ well-defined, and we omit it in the following.) See [MT21, Section 6D] for a detailed account.

Example 3C.5. Here is an example of a left justification:

$$S = \begin{array}{c} i_1 \quad i_2 \quad i_3 \quad i_4 \\ | \quad | \quad | \quad | \\ | \quad | \quad | \quad | \\ i_1 \quad \rho_1 \quad i_2 \quad \rho_2 \quad i_3 \quad \rho_3 \quad i_4 \end{array}, \quad L(S) = \begin{array}{c} \rho_1 \quad i_1 \quad \rho_2 \quad \rho_3 \quad i_3 \quad i_4 \\ | \quad | \quad | \quad | \quad | \quad | \\ | \quad | \quad | \quad | \quad | \quad | \\ i_1 \quad i_2 \quad \rho_2 i_3 \quad i_4 \end{array}.$$

In general, the left justification is obtained by considering a collar neighborhood of a horizontal cut of S . In this neighborhood one inductively pulls the strings to the left. ◇

In a dotted straight line diagram two strings are *close* if you can pull them arbitrarily close to one another using only (bilocal) isotopies. We use *close and to the left/right* in the evident way.

Example 3C.6. Let us repeat [MT21, Example 6D.10]:

$$\begin{array}{c} i \quad j \\ | \quad | \\ | \quad | \\ i \quad j \end{array}, \quad \begin{array}{c} i \quad j \\ | \quad | \\ | \quad | \\ i \quad k \end{array}.$$

The solid i -string is close to the solid j -string in the left but not in the right diagram. ◇

One of the other crucial points about weighted KLRW algebras is that they generalize KLR algebras, see [MT21, Section 3F]. The construction given therein uses a *KLRW positioning*, which is a certain $\mathbf{x} \in X$, and then the KLR algebra is graded isomorphic to $\mathbf{1}_{\mathbf{x}} \mathscr{W}_\beta^\rho(X) \mathbf{1}_{\mathbf{x}}$ where $\mathbf{1}_{\mathbf{x}} = \sum_{\mathbf{i} \in I} \mathbf{1}_{\mathbf{x}, \mathbf{i}}$. We return to this point in Section 5G below.

3D. A basis and a faithful module. The following *standard basis* proposition works only in the infinite dimensional case. One of the main features of our approach is that we can use it to prove cellularity of the finite dimensional quotients as well.

Proposition 3D.1. *The algebra $\mathscr{W}_n^\rho(X)$ is free as an R -module with homogeneous basis*

$$\mathcal{B}_\beta = \{D(w)y_1^{a_1} \dots y_n^{a_n} \mathbf{1}_{\mathbf{x}, \mathbf{i}} \mid a_1, \dots, a_n \in \mathbb{Z}_{\geq 0}, w \in \mathfrak{S}_n, \mathbf{x}, \mathbf{y} \in X, \mathbf{i} \in I^n\}.$$

Proof. See [MT21, Proposition 3B.12] for details. □

Remark 3D.2. The proof of Proposition 3D.1 in [MT21] uses a faithful action on

$$P_n(X) = \bigoplus_{\mathbf{x} \in X, \mathbf{i} \in I^n} R[y_1, \dots, y_n] \mathbf{1}_{\mathbf{x}, \mathbf{i}}.$$

We will not recall the action here as it is quite standard in the field, see [MT21, Section 3C] for details.

4. THE STRATEGY

As we now recall, our strategy to construct homogeneous (affine) sandwich cellular bases for the weighted KLRW algebras is the same as in [MT21, Remark 6.1].

Remark 4A.1. A crucial ingredient is the idea of using a certain form of *minimality*:

- (a) First, construct an idempotent diagram $\mathbf{1}_\lambda$ by placing strings inductively as far to the right as possible, called *placing strings to the right*. Here we use that (3A.3) only allows strings to be pulled to the right in certain situations, such as when they carry a dot. In this way we think of previously placed strings as keeping a new one in check. This ensures that $\mathbf{1}_\lambda$ is minimal with respect to placing the strings to the right. In fact, this strategy is a greedy algorithm, as it is designed to be locally minimal but it produces a globally minimal diagram.

- (b) By (3A.3) again, the diagram $\mathbf{1}_\lambda$ stays minimal when dots are put on certain strands, but putting dots on other strings allows the strings or the dots to move further to the right. So without violating minimality we can place more dots on some strings in $\mathbf{1}_\lambda$ to obtain minimal diagrams of the form $y^a y^f y_\lambda \mathbf{1}_\lambda$, which form the *middle* of the homogeneous (affine) sandwich cellular basis.
- (c) The (sandwich) cellular basis is then obtained by a standard construction for diagram algebras, which in our case means putting semistandard permutation diagrams above and below $y^a y^f y_\lambda \mathbf{1}_\lambda$.
- (d) The basis itself is minimal, by construction, and it is not hard to prove that it is indeed a homogeneous (affine) sandwich cellular basis. For example, putting additional dots on the basis elements allows one pull strings and jump dots to the right, making the result bigger. This gives an inductive way of proving results.

This strategy works perfectly in types A_Z and $A_e^{(1)}$, and requires some small adjustments in other types.

The following lemmas are the crucial diagrammatic relations that we need to pull strings and jump dots to the right. Here we are pulling the leftmost string to the right or jumping the leftmost jump dot to the right. We highlight the strings where the action happens by coloring them.

Lemma 4A.2. *For any quiver and any choice of Q -polynomials we have the following, plus partner relations:*

$$(4A.3) \quad \begin{array}{c} | \\ i \end{array} \begin{array}{c} | \\ i \end{array} = \begin{array}{c} \color{blue}{\diagup} \\ i \end{array} \begin{array}{c} \color{blue}{\diagdown} \\ i \end{array} - \begin{array}{c} \color{blue}{\diagdown} \\ i \end{array} \begin{array}{c} \color{blue}{\diagup} \\ i \end{array}, \quad \begin{array}{c} | \\ i \end{array} \begin{array}{c} | \\ i \end{array} = \begin{array}{c} | \\ i \end{array} \begin{array}{c} | \\ i \end{array} + \begin{array}{c} \color{blue}{\diagup} \\ i \end{array} \begin{array}{c} \color{blue}{\diagdown} \\ i \end{array} - \begin{array}{c} \color{blue}{\diagdown} \\ i \end{array} \begin{array}{c} \color{blue}{\diagup} \\ i \end{array}.$$

For $i \rightarrow j$ edges and the choice of Q -polynomials in (3A.1) we have the following, plus partner relations:

$$(4A.4) \quad \begin{array}{c} \color{green}{\bullet} \\ | \\ i \end{array} \begin{array}{c} | \\ j \end{array} = \begin{array}{c} \color{green}{\bullet} \\ \color{blue}{\diagup} \\ i \end{array} \begin{array}{c} \color{blue}{\diagdown} \\ j \end{array} + \begin{array}{c} | \\ i \end{array} \begin{array}{c} \color{blue}{\bullet} \\ | \\ j \end{array}, \quad \begin{array}{c} | \\ i \end{array} \begin{array}{c} | \\ i \end{array} \begin{array}{c} | \\ j \end{array} \begin{array}{c} | \\ j \end{array} = - \begin{array}{c} \color{blue}{\diagup} \\ i \end{array} \begin{array}{c} \color{blue}{\diagdown} \\ i \end{array} \begin{array}{c} \color{blue}{\bullet} \\ | \\ j \end{array} - \begin{array}{c} \color{blue}{\diagdown} \\ i \end{array} \begin{array}{c} \color{blue}{\diagup} \\ i \end{array} \begin{array}{c} \color{blue}{\bullet} \\ | \\ j \end{array}.$$

The right relation and its partner also hold for $i \leftarrow j$.

For $i \Rightarrow j$ edges and the choice of Q -polynomials in (3A.1) we have the following, plus partner relations:

$$(4A.5) \quad \begin{array}{c} \color{green}{\bullet} \\ | \\ i \end{array} \begin{array}{c} | \\ j \end{array} = \begin{array}{c} \color{green}{\bullet} \\ \color{blue}{\diagup} \\ i \end{array} \begin{array}{c} \color{blue}{\diagdown} \\ j \end{array} + \begin{array}{c} | \\ i \end{array} \begin{array}{c} \color{blue}{\bullet} \\ | \\ j \end{array}.$$

Proof. As in [MT21, Lemmas 6D.1, 6D.4 and 7E.1]. □

The relations (4A.4) and (4A.5) motivate the dot placement in Definition 5D.2 below.

Lemma 4A.6. *For $i \neq j$ and the choice of Q -polynomials in (3A.1) we have the following. In any close situation of the form*

$$\begin{array}{c} | \\ j \end{array} \begin{array}{c} | \\ i \end{array} \begin{array}{c} | \\ i \end{array},$$

we can pull the marked string further to the right. Similarly for its partner relations.

Proof. We first use (4A.3) to create a dot on the now middle ghost i -string. If $i \neq j$ are not connected, then either a plain Reidemeister II relation applies, or either of (4A.4) and (4A.5) apply. In any case, we can pull the leftmost solid i -string to the right. □

The next example should be compared with Remark 5C.7 below.

Example 4A.7. The following close configurations and their partners are stuck for $i \Rightarrow j$ respectively for $i \leftarrow j$, so that Lemma 4A.2 and Lemma 4A.6 do not apply:

$$i \Rightarrow j: \begin{array}{c} | \\ j \end{array} \begin{array}{c} | \\ j \end{array} \begin{array}{c} | \\ i \end{array}, \quad i \leftarrow j: \begin{array}{c} | \\ j \end{array} \begin{array}{c} | \\ i \end{array} \begin{array}{c} | \\ i \end{array}.$$

These configurations will appear whenever i correspond to a leaf of Γ . ◇

5. THE BASES

We now explain the main constructions of this paper. In [Remark 6A.10](#) we summarize the parts of the arguments that are general and those that depend on the underlying quiver.

5A. Some notation. We fix some conventions.

Notation 5A.1. We will use *affine red strings* in diagrams, illustrated by:

$$\text{genuine red string : } \begin{array}{c} | \\ | \\ | \\ \hline | \\ | \\ | \end{array}, \quad \text{affine red string : } \begin{array}{c} | \\ | \\ | \\ \hline | \\ | \\ | \end{array}.$$

Note that affine red strings are not part of the diagrams and they are drawn only as a visual aid.

Notation 5A.2. Unless we are in specific example, we fix arbitrary $n, \ell \in \mathbb{Z}_{\geq 0}$, $e \in \mathbb{Z}_{\geq 2}$, $\kappa \in \mathbb{Z}^\ell$, with $\kappa_1 < \dots < \kappa_\ell$, and $\rho \in I^\ell$ for the duration. We let

$$\underline{\ell} = \ell + n(e + 1)$$

be the *affine level*. More generally, we will use the underline notation to indicate definitions that only play a role for the affine case.

Notation 5A.3. Our constructions given in this section work for the quivers below.

- (a) We use Kac's notation [[Kac90](#)] for Dynkin quivers (but we mirrored the quivers left-to-right). The main quivers of study in this paper are:

$$(5A.4) \quad \begin{array}{l} B_{\mathbb{Z}_{\geq 0}} : \quad \bullet \leftarrow \bullet \text{---} \bullet \text{---} \bullet \text{---} \bullet \text{---} \bullet \text{---} \bullet \text{---} \bullet \cdots, \\ A_{2,e}^{(2)} : \quad \bullet \text{---} \bullet \text{---} \bullet \text{---} \bullet \cdots \bullet \text{---} \bullet \text{---} \bullet \text{---} \bullet, \\ D_{e+1}^{(2)} : \quad \bullet \leftarrow \bullet \text{---} \bullet \text{---} \bullet \cdots \bullet \text{---} \bullet \text{---} \bullet \text{---} \bullet, \end{array}$$

where $e \in \mathbb{Z}_{\geq 2}$. Here we orient the simply laced edges $i \rightarrow (i + 1)$. We will omit $B_{\mathbb{Z}_{\geq 0}}$ from the discussion: this type can be viewed as $D_{e+1}^{(2)}$ for $e \rightarrow \infty$, but doing so needs some (harmless) adjustments of the exposition since e.g. the affine level would be infinite.

- (b) Let $0 < \varepsilon < \frac{1}{4n\underline{\ell}}$ be a small shift. We let the ghost shifts for edges in BAD types be 1 with the exception of the edge $0 \leftarrow 1$ in type $D_{e+1}^{(2)}$ where the ghost shift is $1 - \varepsilon^2$.

Definition 5A.5. A *sink* is a vertex of a Dynkin quiver Γ that is a (graph-theoretical) sink. A *multisink* is a sink with only adjacent multi-laced edges.

Note that, if i is a sink, then the solid i -strings do not have ghosts.

Example 5A.6. The vertex e is a multisink for BAD types, and the vertex 0 is additionally a multisink for type $D_{e+1}^{(2)}$. With contrast, in type $C_e^{(1)}$ no vertex is a multisink, but some vertices are sinks. \diamond

In type $D_{e+1}^{(2)}$ the solid 1-string has two ghosts that are very close to one another by our choice of ghost shifts. We display these two 1-ghosts as doubled lines:

$$\begin{array}{c} | \\ | \\ | \\ \hline | \\ | \\ | \end{array} \quad \begin{array}{c} 11 \\ \vdots \\ \vdots \\ \vdots \end{array} \rightsquigarrow \begin{array}{c} | \\ | \\ | \\ \hline | \\ | \\ | \end{array} \quad \begin{array}{c} 1 \\ \vdots \\ \vdots \\ \vdots \end{array}.$$

We stress that these are two different ghost 1-strings, cf. [Remark 3A.5](#).

Notation 5A.7. We will draw diagrams that are supposed to make sense in any type, but the reader may need to remove or double some ghost strings to obtain the required diagram for a particular type.

Definition 5A.8. Define the *affine charge* $\underline{\kappa} = (\kappa_1, \dots, \kappa_\ell) \in \mathbb{Z}^\ell$ and the *affine red labels* $\underline{\rho} = (\rho_1, \dots, \rho_\ell) \in I^\ell$ by

$$\underline{\kappa}_m = \begin{cases} \kappa_m & \text{if } 1 \leq m \leq \ell, \\ \kappa_\ell + 2n(m - \ell) & \text{otherwise,} \end{cases} \quad \text{and} \quad \underline{\rho}_m = \begin{cases} \rho_m & \text{if } 1 \leq m \leq \ell, \\ \lfloor \frac{m-\ell-1}{n} \rfloor + (e+1)\mathbb{Z} & \text{otherwise.} \end{cases}$$

We call $\underline{\kappa}_m$ and $\underline{\rho}_m$ the *position and residue* of a red string for $m \leq \ell$, and the *position and residue* of an affine red string for $m > \ell$.

Note that the coordinates of the (affine) red strings $\underline{\kappa}$ are always integers.

Example 5A.9. Take $n = 3$, $e = 2$ and $\ell = 1$, so $\underline{\ell} = 1 + 3 \cdot (2 + 1) = 10$. If $\underline{\kappa} = (2)$ and $\underline{\rho} = (1)$, then $\underline{\kappa} = (2, 8, 14, 20, 26, 32, 38, 44, 50, 56)$ and $\underline{\rho} = (1, 0, 0, 0, 1, 1, 1, 2, 2, 2)$. All entries, of $\underline{\kappa}$ and of $\underline{\rho}$, except the first are affine. \diamond

5B. Partition combinatorics. Before coming to our main definitions, we introduce the tableaux combinatorics that arise in BAD types. For the standard tableaux combinatorics that appears in the context of KLR algebras we refer the reader to [HM10, Section 3.3].

Remark 5B.1. The partition combinatorics that we use is motivated by e.g. [AP14] and [AP16]. The associated weighted KLRW diagram combinatorics is a slight modification of the combinatorics of type $C_e^{(1)}$ as in [MT21, Section 7]. The reader should be careful because, as we will see, the partition combinatorics depends on $\underline{\rho}$. In particular, the combinatorics from [AP14] and [AP16] only applies for cyclotomic KLR algebras for the fundamental weights associated to multisink vertices.

Identify the vertices of I with $\mathbb{Z}/(e+1)\mathbb{Z}$. We use (*usual*) *partitions* of n , following the same conventions as in [MT21, Section 6A]. We also use *shifted partitions* of n , that is, partitions λ with strictly decreasing components $\lambda = (\lambda_1 > \dots > \lambda_k)$. Let $|\lambda|$ be the *size* of a partition or shifted partition.

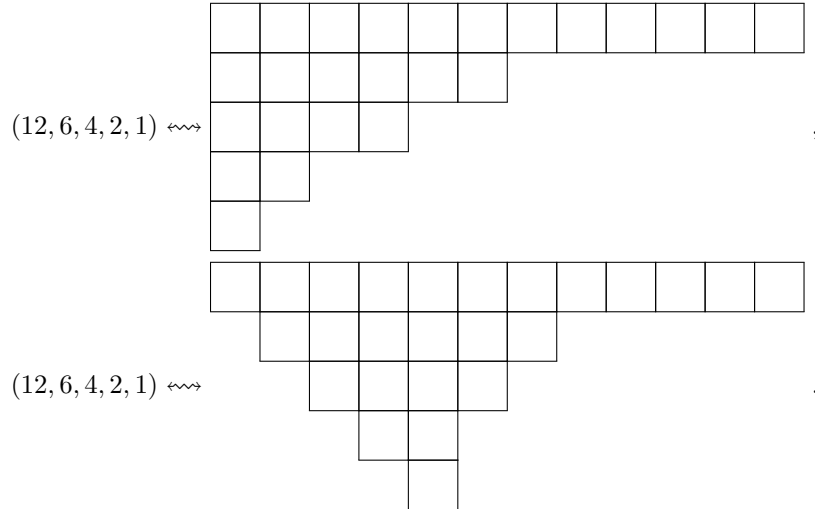
Definition 5B.2. The set of $\underline{\rho}$ -partitions is

$$\mathbb{P}_{\underline{\rho}, n}^{\underline{\rho}} = \left\{ (\lambda^{(1)} | \dots | \lambda^{(\ell)}) \mid \begin{array}{l} |\lambda^{(1)}| + \dots + |\lambda^{(\ell)}| = n, \text{ where} \\ \lambda^{(i)} \text{ is a usual partition if } \rho_i \text{ is not a multisink} \\ \lambda^{(i)} \text{ is a shifted partition if } \phi_i \text{ is a multisink} \end{array} \right\}$$

We identify a $\underline{\rho}$ -partition λ with its *shifted $\underline{\rho}$ -Young diagram*, which is the set of nodes $\{(m, r, c)\}$ where $1 \leq m \leq \ell$, $\lambda_r^{(m)} > 0$, and

$$\begin{cases} 1 \leq c \leq \lambda_r^{(m)} & \text{if } \rho_m \text{ is not a multisink,} \\ 1 + r \leq c \leq \lambda_r^{(m)} + r & \text{if } \rho_m \text{ is a multisink.} \end{cases}$$

Notation 5B.3. We use the (shifted) English convention to illustrate the associated (*shifted*) $\underline{\rho}$ -Young diagrams. That is, we illustrate these partitions by drawing them as boxes in the plane, with rows ordered from top to bottom, and columns left to right, and where the r th row is shifted r positions to the right for shifted $\underline{\rho}$ -Young diagrams. (So the c th column of the r th row is in position $c + r$.) For example, a usual Young diagram and a shifted Young diagram are



This is a different convention to that used in [MT21, Sections 6 and 7] where the Russian convention is used. The Russian convention is useful in types $A_{\mathbb{Z}}$ and $A_e^{(1)}$, but it irrelevant in other types.

That is, if ρ_i corresponds to a multisink vertex (i.e. the vertices e in BAD types and additional the vertex 0 in type $D_{e+1}^{(2)}$), then we consider shifted partitions in the i th entry of λ , and usual partitions otherwise. We make similar definitions as above for $\underline{\rho}$ -partitions. The nodes for $m > \ell$ are called *affine nodes*. Identify $\mathbb{P}_{\underline{\rho}, n}^{\underline{\rho}}$ consisting of the $\underline{\rho}$ that do not contain any affine nodes.

Definition 5B.4. Let $a = 1$ for type $A_{2e}^{(2)}$ and $a = 2$ for type $D_{e+1}^{(2)}$. Given an integer $k \in \mathbb{Z}$ we need the remainder of division by $2e + a$ (viewed as an element in $\{0, \dots, 2e + a\} \subset \mathbb{Z}_{\geq 0}$) which we denote by

$\text{Mod}(k, 2e + a)$. Define the **residue function** $r: \mathbb{Z} \rightarrow I$ by

$$r(k) = \begin{cases} \text{Mod}(k, 2e + a) + (e + 1)\mathbb{Z} & \text{if } 0 \leq \text{Mod}(k, 2e + a) \leq e, \\ 2e + 1 - \text{Mod}(k, 2e + a) + (e + 1)\mathbb{Z} & \text{if } e < \text{Mod}(k, 2e + a) < 2e + a. \end{cases}$$

The $(\underline{\rho})$ -**residue** of the node (m, r, c) is $\text{res}_\rho(m, r, c) = r(c - r) + \rho_m + (e + 1)\mathbb{Z}$.

In illustrations we will often fill nodes with their residues.

Example 5B.5. For $\lambda = (10, 9, 8, 7, 6, 5, 4)$ and $e = 3$, starting with 0, i.e. $\rho = (3)$, we get:

$$A_{2,3}^{(2)} : \begin{array}{cccccccccc} 3 & 2 & 1 & 0 & 1 & 2 & 3 & 3 & 2 & 1 \\ & 3 & 2 & 1 & 0 & 1 & 2 & 3 & 3 & 2 \\ & & 3 & 2 & 1 & 0 & 1 & 2 & 3 & 3 \\ & & & 3 & 2 & 1 & 0 & 1 & 2 & 3 \\ & & & & 3 & 2 & 1 & 0 & 1 & 2 \\ & & & & & 3 & 2 & 1 & 0 & 1 \\ & & & & & & 3 & 2 & 1 & 0 \end{array}, \quad D_{3+1}^{(2)} : \begin{array}{cccccccccc} 3 & 2 & 1 & 0 & 0 & 1 & 2 & 3 & 3 & 2 \\ & 3 & 2 & 1 & 0 & 0 & 1 & 2 & 3 & 3 \\ & & 3 & 2 & 1 & 0 & 0 & 1 & 2 & 3 \\ & & & 3 & 2 & 1 & 0 & 0 & 1 & 2 \\ & & & & 3 & 2 & 1 & 0 & 0 & 1 \\ & & & & & 3 & 2 & 1 & 0 & 0 \\ & & & & & & 3 & 2 & 1 & 0 \end{array}.$$

Note that colored/shaded residues, for multisinks, are doubled. In words, the residues increase along rows and columns until they hit e , this value is doubled, and then the residues bounce back until they hit 0, this value is doubled for $D_{e+1}^{(2)}$, and the process starts again.

In contrast, if $\rho = (1)$, then

$$A_{2,3}^{(2)} : \begin{array}{cccccccccc} 1 & 2 & 3 & 3 & 2 & 1 & 0 & 1 & 2 & 3 \\ & 0 & 1 & 2 & 3 & 3 & 2 & 1 & 0 & 1 \\ & & 1 & 0 & 1 & 2 & 3 & 3 & 2 & 1 \\ & & & 2 & 1 & 0 & 1 & 2 & 3 & 3 \\ & & & & 3 & 2 & 1 & 0 & 1 & 2 \\ & & & & & 3 & 3 & 2 & 1 & 0 \\ & & & & & & 2 & 3 & 3 & 2 \end{array}, \quad D_{3+1}^{(2)} : \begin{array}{cccccccccc} 1 & 2 & 3 & 3 & 2 & 1 & 0 & 0 & 1 & 2 \\ & 0 & 1 & 2 & 3 & 3 & 2 & 1 & 0 & 0 \\ & & 0 & 0 & 1 & 2 & 3 & 3 & 2 & 1 \\ & & & 1 & 0 & 0 & 1 & 2 & 3 & 3 \\ & & & & 2 & 1 & 0 & 0 & 1 & 2 \\ & & & & & 3 & 2 & 1 & 0 & 0 \\ & & & & & & 2 & 3 & 3 & 2 \end{array},$$

following [Definition 5B.2](#). For $\rho = (2)$ the situation is similar, and for $\rho = (0)$ type $A_{2,3}^{(2)}$ has usual and type $D_{3+1}^{(2)}$ shifted partition combinatorics. We emphasize that, in general, there are more usual partitions than shifted partitions so there are more of these diagrams when ρ_i is not a multisink \diamond

The coloring/shading from [Example 5B.5](#) also distinguishes between usual and shifted partition combinatorics: we are in the case of the shifted combinatorics if and only if the first node is colored/shaded.

Example 5B.6. We continue with [Example 5A.9](#) and fix type $A_{2,2}^{(2)}$. There are three usual and two shifted 1-partitions of 3 and eight in total, namely (filled with their residues):

$$\begin{aligned} \lambda_1 &= \begin{array}{|c|c|c|} \hline 0 & 1 & 2 \\ \hline \end{array}, & \lambda_2 &= \begin{array}{|c|c|} \hline 0 & 1 \\ \hline 1 & \\ \hline \end{array}, & \lambda_3 &= \begin{array}{|c|} \hline 0 \\ \hline 1 \\ \hline 2 \\ \hline \end{array}, \\ \mu_1 &= \begin{array}{|c|c|c|} \hline 1 & 2 & 2 \\ \hline \end{array}, & \mu_2 &= \begin{array}{|c|c|} \hline 1 & 2 \\ \hline 0 & \\ \hline \end{array}, & \mu_3 &= \begin{array}{|c|} \hline 1 \\ \hline 0 \\ \hline 1 \\ \hline \end{array}, \\ \nu_1 &= \begin{array}{|c|c|c|} \hline 2 & 1 & 0 \\ \hline \end{array}, & \nu_2 &= \begin{array}{|c|c|} \hline 2 & 1 \\ \hline & 2 \\ \hline \end{array}. \end{aligned}$$

We get $P_{\ell,n}^\rho = \{\lambda_1, \lambda_2, \lambda_3\}$, if $\rho = (0)$, $P_{\ell,n}^\rho = \{\mu_1, \mu_2, \mu_3\}$, if $\rho = (1)$, and $P_{\ell,n}^\rho = \{\nu_1, \nu_2\}$, for $\rho = (2)$.

The set $\underline{P}_{\ell,n}^{\rho,all}$ is much bigger, and we will not list it here. Note however that the affine components of $\underline{P}_{\ell,n}^{\rho,all}$ have either usual or shifted partition combinatorics. Precisely, since $\underline{\rho} = (\rho, 0, 0, 0, 1, 1, 1, 2, 2, 2)$ we get that the first six affine components of $\underline{P}_{\ell,n}^{\rho,all}$ have usual and the last three have shifted partition combinatorics. \diamond

Remark 5B.7. In examples and also proofs below we will mostly focus on the shifted partition combinatorics. The situation for the usual partition combinatorics is then a slight adjustment of that used for type $C_e^{(1)}$ in [MT21, Section 7].

5C. The (dotted) idempotent. We now introduce some crucial definitions. For any $r + (e + 1)\mathbb{Z} \in I$ with $r \in \{0, \dots, e\}$ we sometimes abuse notation and identify $(r + (e + 1)\mathbb{Z})$ for the associated real number in $r \in \mathbb{R}$.

Definition 5C.1. Define the **content function** (for the m th component) $c^m : I \rightarrow \mathbb{R}$ by

$$c^m(r) = \begin{cases} 2 - \rho_m & \text{if } \rho_m \neq 0, r = 0 \text{ and we are in type } D_{e+1}^{(2)}, \\ r - 2 & \text{if } \rho_m = 0, r \neq 0 \text{ and we are in type } D_{e+1}^{(2)}, \\ r - \rho_m & \text{otherwise.} \end{cases}$$

Recall the shift ε from [Notation 5A.3](#). We now define the **positioning function**, which uses the **row reading order** $p_{\lambda}(m, r, c) = c + \sum_{i=1}^{r-1} \lambda_i^{(m)}$. (The function $p_{\lambda}(-)$ returns the position of a node in a Young diagram when reading along rows, i.e. reading first left to right, and then bottom to top. So $p_{\lambda}(m, r, c) = k$ if (m, r, c) is the k th node in row reading order.) From now on we always order nodes and strings by the row reading order.

Definition 5C.2. Let $\lambda \in \underline{P}_{\ell,n}^{\rho,all}$. The **coordinate** of $(m, r, c) \in \lambda$ with $p_{\lambda}(m, r, c) = k$, is

$$x_{\kappa}(m, r, c) = \kappa_m - \frac{m}{\ell} + c^m(r(k)) - k\varepsilon.$$

The **coordinates** $x_{\kappa}(\lambda)$ of λ is the ordered tuple of the coordinates of its nodes listed in row reading order.

[Definition 5C.2](#) looks more complicated than it actually is. The coordinate function simply places strings in order, following the strategy outlined in [Remark 4A.1](#).

Remark 5C.3. The contributions of the ingredients of $x_{\kappa}(m, r, c)$ are the following:

- (a) κ_m is the coordinate where the nodes for the component $\lambda^{(m)}$ are centered.
- (b) The $\frac{m}{\ell}$ differentiates between the components.
- (c) $c^m(r(k))$ ensures that strings with the same residue are placed within a certain region. The first two cases in the definition of c^m takes care of the 0 multisinks, which have special combinatorics, and the shift by ρ_m ensures that coordinates of residue ρ_m are the rightmost coordinates.
- (d) $-k\varepsilon$ ensures that nodes move a little bit to the left as we read along rows.

Note that in type $D_{e+1}^{(2)}$ the solid 0-strings and the solid 2-strings have roughly the same coordinates. This is important because the solid 0-strings do not have associated ghosts, but the solid 1-strings have two associated ghosts.

Example 5C.4. We continue with [Example 5B.6](#). Fix from now on $\kappa = (0)$. We have the following coordinates of ν_1 and ν_2 :

$$\begin{aligned} x_{\kappa}(\nu_1) &= (-\varepsilon, -1 - 2\varepsilon, -2 - 3\varepsilon), & \begin{array}{|c|c|c|} \hline -\varepsilon & -1-2\varepsilon & -2-3\varepsilon \\ \hline \end{array} & \xrightarrow{\varepsilon \rightarrow 0} & \begin{array}{|c|c|c|} \hline 0 & -1 & -2 \\ \hline \end{array}, \\ x_{\kappa}(\nu_2) &= (-\varepsilon, -1 - 2\varepsilon, -3\varepsilon), & \begin{array}{|c|c|} \hline -\varepsilon & -1-2\varepsilon \\ \hline & -3\varepsilon \\ \hline \end{array} & \xrightarrow{\varepsilon \rightarrow 0} & \begin{array}{|c|c|} \hline 0 & -1 \\ \hline & 0 \\ \hline \end{array}. \end{aligned}$$

We have illustrated the coordinates for the nodes in the shifted Young diagrams, and also what happens in the limit $\varepsilon \rightarrow 0$. Note that we have omitted the additional shift of $\frac{m}{\ell} = \frac{1}{10}$. \diamond

We write $x_{\kappa}(f)$ for the maximum of x_{κ} on $P_{\ell,n}^{\rho}$, and call coordinates with $x_{\kappa}(m, r, c) > x_{\kappa}(f)$ **affine**.

Lemma 5C.5. *The nodes with affine coordinates are precisely the affine nodes.*

Proof. Easy and omitted. \square

We now define the **(dotted) idempotent diagrams** $\mathbf{1}_{\lambda}$ and $\mathbf{1}_{\lambda}^y$ associated to $\lambda \in \underline{P}_{\ell,n}^{\rho,all}$.

Definition 5C.6. For $\lambda \in \underline{P}_{\ell,n}^{\rho,all}$ let $\mathbf{1}_\lambda$ be the idempotent diagram given by

- (a) placing ℓ red strings with labels given by ρ at coordinates given by κ , and,
- (b) n solid strings with labels $\text{res}_\rho(m, r, c)$ at coordinates $\mathbf{x}_\kappa(m, r, c)$, for $(m, r, c) \in \lambda$.

As mentioned already, in diagrams we will also draw affine red strings at positions κ_m for $\ell < m \leq \ell$.

Remark 5C.7. In AC types the crucial illustrations that we used to show that our bases span are [MT21, (6A.10), (6A.11), (7A.8), (7A.9) and (7A.10)]. These diagrams identify local configurations of nodes in Young diagrams with local configurations of strings in diagrams. Their analogs, illustrating the residues in the nodes, are as follows.

Assuming that the middle node is not 0 or e and we do not have $i - 2 = 0$, $i = 0$ or $i + 2 = 0$ in type $D_{e+1}^{(2)}$, we have:

$$(5C.8) \quad \begin{array}{|c|c|c|} \hline i & i+1 & i+2 \\ \hline \end{array} \longleftrightarrow \begin{array}{c} | \\ i \\ \hline \end{array} \begin{array}{c} | \\ i+1 \\ \hline \end{array} \begin{array}{c} | \\ i+2 \\ \hline \end{array}, \quad \begin{array}{|c|c|c|} \hline i & i-1 & i-2 \\ \hline \end{array} \longleftrightarrow \begin{array}{c} | \\ i-2 \\ \hline \end{array} \begin{array}{c} | \\ i-1 \\ \hline \end{array} \begin{array}{c} | \\ i \\ \hline \end{array}.$$

The special cases in Definition 5C.1 for type $D_{e+1}^{(2)}$ correspond to:

$$(5C.9) \quad \begin{array}{|c|c|c|} \hline 0 & 1 & 2 \\ \hline \end{array} \longleftrightarrow \begin{array}{c} | \\ 1 \\ \hline \end{array} \begin{array}{c} | \\ 20 \\ \hline \end{array} \begin{array}{c} | \\ 2 \\ \hline \end{array}, \quad \begin{array}{|c|c|c|} \hline 2 & 1 & 0 \\ \hline \end{array} \longleftrightarrow \begin{array}{c} | \\ 1 \\ \hline \end{array} \begin{array}{c} | \\ 02 \\ \hline \end{array} \begin{array}{c} | \\ 2 \\ \hline \end{array}.$$

That the two cases in (5C.8) and (5C.9) look different is an artifact of our conventions for ghost strings. However, this can not be avoided (meaning that one always gets special behavior) in type $D_{e+1}^{(2)}$ as there is no way to orient the quiver from left to right, or right to left.

When the middle residue is 0 or e we have:

$$(5C.10) \quad \begin{array}{|c|c|c|} \hline 1 & 0 & 1 \\ \hline \end{array} \longleftrightarrow \begin{array}{c} | \\ 0 \\ \hline \end{array} \begin{array}{c} | \\ 11 \\ \hline \end{array} \begin{array}{c} | \\ 11 \\ \hline \end{array}, \quad \begin{array}{|c|c|c|c|} \hline 1 & 0 & 0 & 1 \\ \hline \end{array} \longleftrightarrow \begin{array}{c} | \\ 1 \\ \hline \end{array} \begin{array}{c} | \\ 1 \\ \hline \end{array} \begin{array}{c} | \\ 00 \\ \hline \end{array} \begin{array}{c} | \\ 1 \\ \hline \end{array}, \\ \begin{array}{|c|c|c|c|} \hline e-1 & e & e & e-1 \\ \hline \end{array} \longleftrightarrow \begin{array}{c} | \\ e-1 \\ \hline \end{array} \begin{array}{c} | \\ e-1 \\ \hline \end{array} \begin{array}{c} | \\ e \\ \hline \end{array} \begin{array}{c} | \\ e \\ \hline \end{array}.$$

These should be compared to Example 4A.7.

Whenever we have a multisink Remark 4A.1.(b) fails because (3A.3) annihilates the diagram. In Definition 5C.12 below, we will place a dot on the strands to avoid this.

Finally (note that $|i - j| \leq 1$ in these pictures):

$$(5C.11) \quad \begin{array}{|c|c|c|c|} \hline k \mp 1 & \dots & j & i \\ \hline k & & & \\ \hline \end{array} \quad \text{or} \quad \begin{array}{|c|c|c|c|} \hline k & \dots & j & i \\ \hline & k & & \\ \hline \end{array} \longleftrightarrow \left\{ \begin{array}{l} \begin{array}{c} | \\ i \\ \hline \end{array} \begin{array}{c} | \\ i \\ \hline \end{array} \begin{array}{c} | \\ i \\ \hline \end{array} \begin{array}{c} | \\ i \\ \hline \end{array} \begin{array}{c} | \\ i \\ \hline \end{array} \begin{array}{c} | \\ i \\ \hline \end{array} \\ \text{if } i = k = j \\ \text{is a multisink,} \\ \\ \begin{array}{c} | \\ i \\ \hline \end{array} \begin{array}{c} | \\ i \\ \hline \end{array} \begin{array}{c} | \\ i \\ \hline \end{array} \\ \text{if } i = k \neq j, \\ \\ \begin{array}{c} | \\ i \\ \hline \end{array} \begin{array}{c} | \\ k \\ \hline \end{array} \begin{array}{c} | \\ k \\ \hline \end{array} \begin{array}{c} | \\ i \\ \hline \end{array} \quad \text{or} \quad \begin{array}{c} | \\ k \\ \hline \end{array} \begin{array}{c} | \\ i \\ \hline \end{array} \begin{array}{c} | \\ i \\ \hline \end{array} \\ \text{if } |k - i| = 1, \\ \\ \text{the solid/ghost } k\text{-string is close} \\ \text{to a ghost/solid } (k \pm 1)\text{-string} \quad \text{otherwise,} \end{array} \right.$$

where the j -string is only illustrated in the top diagram, and in the last case the i and k -strings do not need to be close (neither the solids nor the ghosts). Note that in the shifted Young diagram $k = \rho_k$.

Definition 5C.12. Suppose $\lambda \in \underline{P}_{\ell,n}^{\rho,all}$. Set $p_\lambda(m, r, c) = k$ and $p_\lambda(m, r', c') = k + 1$. If ρ_m is not a multisink (so usual partitions), then

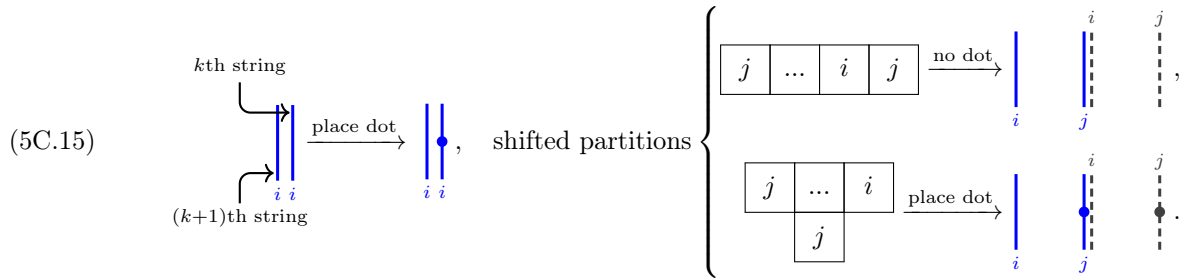
$$(5C.13) \quad a_k = \begin{cases} 1 & \text{if } \text{res}_\rho(m, r, c) = \text{res}_\rho(m, r + 1, 1), \\ 0 & \text{otherwise.} \end{cases}$$

If ρ_m is a multisink (so shifted partitions), then

$$(5C.14) \quad a_k = \begin{cases} 1 & \text{if } \text{res}_\rho(m, r, c) = \text{res}_\rho(m, r', c') \text{ or } (r' > 1, c' = 1), \\ 0 & \text{otherwise.} \end{cases}$$

The *dotted idempotent* associated to λ is $\mathbf{1}_\lambda^y = y_\lambda \mathbf{1}_\lambda$, where $y_\lambda = y_1^{a_1} \dots y_n^{a_n} \in R[y_1, \dots, y_n]$.

In other words, (5C.13) places a dot whenever the k th and the $(k + 1)$ th string are close and have the same residue, and takes care of new rows as in (5C.11), e.g.:



In the case of usual partitions the dot placement is the same as in type $C_e^{(1)}$ from [MT21, Section 7], see also (5C.19) below. Note that $\mathbf{1}_\lambda^y$ has zero or one dot on each strand. For example, the top diagram in (5C.11) gets two dots, one on the middle and one on the rightmost string.

Example 5C.16. We list a few examples of the dotted idempotent $\mathbf{1}_\lambda^y$ for $\ell = 1$ and $\kappa = (0)$.

(a) Consider $\lambda = (9)$ for $e = 3$ and $\rho = (3)$. We get:

$$A_{2,3}^{(2)} : \begin{bmatrix} 3 & 2 & 1 & 0 & 1 & 2 & 3 & 3 & 2 \end{bmatrix}, \quad D_{3+1}^{(2)} : \begin{bmatrix} 3 & 2 & 1 & 0 & 0 & 1 & 2 & 3 & 3 \end{bmatrix}.$$

$$A_{2,3}^{(2)} : \mathbf{1}_\lambda^y = \begin{array}{c} 0 \\ | \\ 0 \end{array}, \quad \begin{array}{c} 0 \\ | \\ 1 \ 1 \end{array}, \quad \begin{array}{c} 1 \ 1 \\ | \ | \\ 2 \ 2 \ 2 \end{array}, \quad \begin{array}{c} 2 \ 2 \ 2 \\ | \ | \ | \\ 3 \ 3 \ 3 \end{array}, \quad \begin{array}{c} 2 \\ | \\ 3 \ 3 \end{array},$$

$$D_{3+1}^{(2)} : \mathbf{1}_\lambda^y = \begin{array}{c} | \\ 1 \ 1 \end{array}, \quad \begin{array}{c} 1 \ 1 \\ | \ | \\ 2 \ 0 \ 0 \ 2 \end{array}, \quad \begin{array}{c} 2 \\ | \\ 3 \ 3 \end{array}, \quad \begin{array}{c} 2 \\ | \\ 3 \ 3 \end{array}.$$

In contrast, if we instead have $\rho = (0)$, then we get

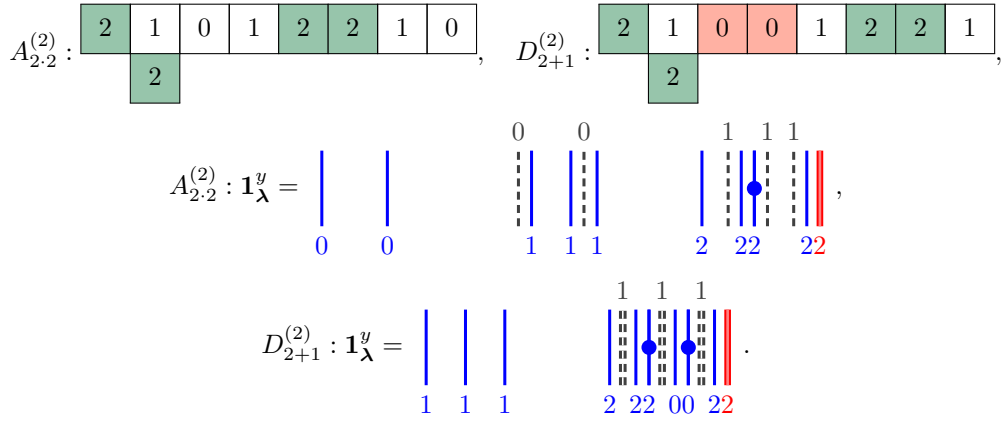
$$A_{2,3}^{(2)} : \begin{bmatrix} 0 & 1 & 2 & 3 & 3 & 2 & 1 & 0 & 1 \end{bmatrix}, \quad D_{3+1}^{(2)} : \begin{bmatrix} 0 & 1 & 2 & 3 & 3 & 2 & 1 & 0 & 0 \end{bmatrix}.$$

$$A_{2,3}^{(2)} : \mathbf{1}_\lambda^y = \begin{array}{c} | \\ 0 \end{array}, \quad \begin{array}{c} | \\ 0 \ 0 \end{array}, \quad \begin{array}{c} 0 \\ | \ | \\ 1 \ 1 \end{array}, \quad \begin{array}{c} 0 \\ | \\ 1 \end{array}, \quad \begin{array}{c} 1 \ 1 \ 1 \\ | \ | \ | \\ 2 \ 2 \end{array}, \quad \begin{array}{c} 2 \ 2 \\ | \ | \\ 3 \ 3 \end{array},$$

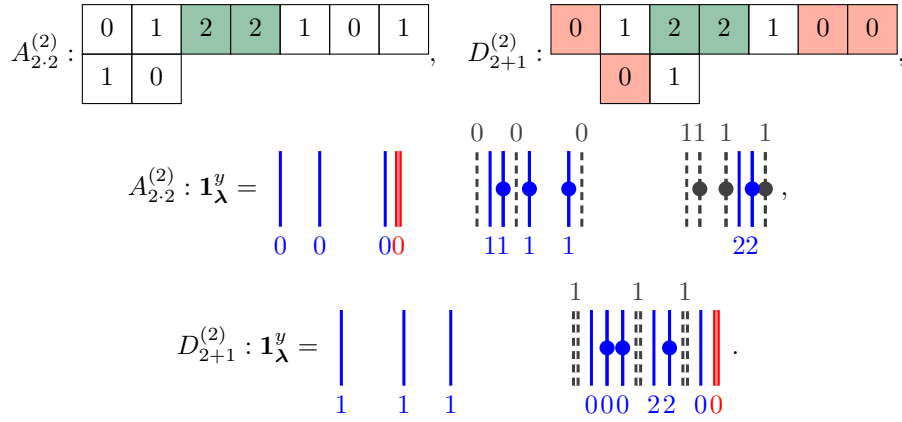
$$D_{3+1}^{(2)} : \mathbf{1}_\lambda^y = \begin{array}{c} | \\ 1 \end{array}, \quad \begin{array}{c} | \\ 1 \end{array}, \quad \begin{array}{c} 1 \ 1 \\ | \ | \\ 0 \ 0 \ 2 \end{array}, \quad \begin{array}{c} 1 \ 1 \\ | \ | \\ 2 \ 0 \ 0 \end{array}, \quad \begin{array}{c} 2 \ 2 \\ | \ | \\ 3 \ 3 \end{array}.$$

Note the different dot placement: for type $A_{2,3}^{(2)}$ we use (5C.13), while for $D_{3+1}^{(2)}$ we use (5C.14).

(b) Next, we illustrate the dotted idempotent for $\lambda = (8, 1)$, $e = 2$ and $\rho = (2)$:



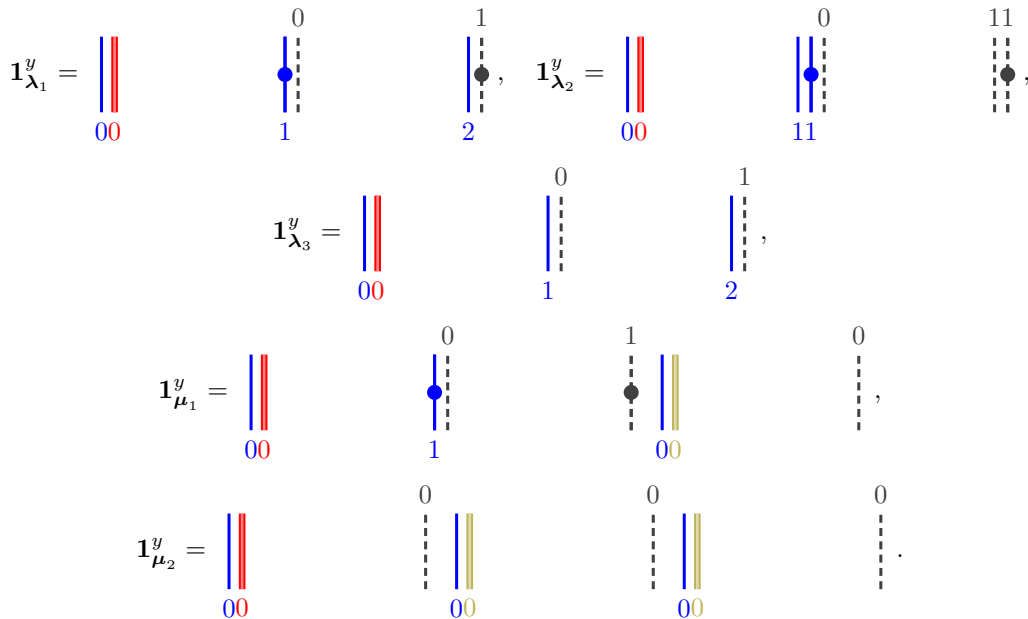
(c) Finally, consider $\lambda = (7, 2)$ for $e = 2$ and $\rho = (0)$. Then:



Again, note the different dot placement for types $A_{2,2}^{(2)}$ and $D_{2+1}^{(2)}$.

All of these pictures were created using a tikz macro defined in the preamble. \diamond

Example 5C.17. We continue with [Example 5C.4](#). Recall that $n = 3$, $e = 2$, $\ell = 1$ and $\kappa = (0)$, and fix $\rho = (0)$. Let us consider $\lambda_1 = (3|\emptyset|\dots|\emptyset)$, $\lambda_2 = (2, 1|\emptyset|\dots|\emptyset)$ and $\lambda_3 = (1^3|\emptyset|\dots|\emptyset)$, and also $\mu_1 = (2|1|\emptyset|\dots|\emptyset)$ and $\mu_2 = (1|1|1|\emptyset|\dots|\emptyset)$. These five diagrams have the following dotted idempotent diagrams for type $A_{2,2}^{(2)}$:



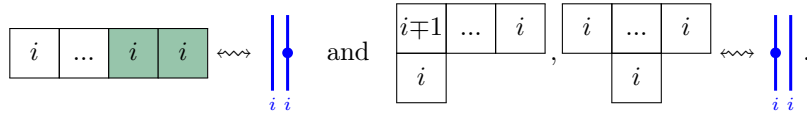
Here we have drawn affine red strings in the final two diagrams. The dotted idempotents for type $D_{e+1}^{(2)}$ look similar, but since there is no ghost 0-string the 1 and 2 strings move to the left. For example

$$\mathbf{1}_{\lambda_1}^y = \begin{array}{c} | \\ | \\ | \\ | \\ | \\ | \\ | \\ | \\ | \\ 1 \end{array} \quad \begin{array}{c} 1 \\ | \\ | \\ | \\ | \\ | \\ | \\ | \\ | \\ | \\ | \\ 2 \ 00 \end{array}$$

illustrates $\mathbf{1}_{\lambda_1}^y$ for type $D_{2+1}^{(2)}$. \diamond

Lemma 5C.18. *We have $\mathbf{1}_{\lambda}^y = \mathbf{1}_{\mu}^y$ if and only if $\lambda = \mu$.*

Proof. One direction is immediate, so let us assume that $\lambda \neq \mu$. If $\text{res}_{\rho}(\lambda) \neq \text{res}_{\rho}(\mu)$, then $\mathbf{1}_{\lambda}^y \neq \mathbf{1}_{\mu}^y$ follows using the faithful polynomial module from Remark 3D.2. Moreover, a different dot placement on the same $\mathbf{1}_{\lambda}$ can also be distinguished by Remark 3D.2, so it remains to argue that $\lambda \neq \mu$ implies a different dot placement if $\text{res}_{\rho}(\lambda) = \text{res}_{\rho}(\mu)$. To see this assume that the k th node is the first node that is different for λ and μ . Without loss of generality, we can assume that the k th node of μ is in a new row when compared to the k th node of λ . There are three cases to check now, depending on the residue j of the k th string and the residue i of the $(k-1)$ th string. When $i = j$ is a multisink the local diagrams for λ and μ are:



The case $i \rightsquigarrow j$ for shifted partitions is illustrated in (5C.15), while

$$(5C.19) \quad \begin{array}{c} j-1 \dots i \ j \\ | \\ | \\ | \\ i \end{array} \xrightarrow{\text{place dot}} \begin{array}{c} i \\ | \\ | \\ | \\ j \end{array}, \quad \begin{array}{c} j \\ | \\ | \\ | \\ j \end{array}, \quad \begin{array}{c} j-1 \dots i \\ j \end{array} \xrightarrow{\text{no dot}} \begin{array}{c} | \\ | \\ | \\ i \end{array}, \quad \begin{array}{c} i \\ | \\ | \\ | \\ j \end{array}, \quad \begin{array}{c} j \\ | \\ | \\ | \\ j \end{array}$$

is the case for usual partitions. The case $i \leftarrow j$ is similar to (5C.15) and (5C.19). \square

5D. The sandwiched part. The following configurations of close strings are needed in Definition 5D.2:

$$(5D.1) \quad \begin{array}{c} i \\ | \\ | \\ | \\ j \end{array} \quad \text{if } i \Rightarrow j.$$

(This diagram does not arise if i has no ghost.) In these illustrations we have highlighted the string that can get a dot in the sandwiched part, which is the leftmost illustrated string.

Definition 5D.2. Define the set of *affine dots* as

$$A^y(\lambda) = \{a = (a_1, \dots, a_n) \in \mathbb{Z}_{\geq 0}^n \mid a_k = 0 \text{ whenever } \mathbf{x}_{\kappa}(\lambda)_k \leq \mathbf{x}_{\kappa}(f)\}.$$

For $1 \leq k \leq n$ define $c_k(\lambda) = 1$ if the k th string is close as in (5D.1) and does not already have a dot in $\mathbf{1}_{\mu}^y$ for some $\mu \in \underline{P}_{\ell, n}^{all}$ with $\mathbf{1}_{\lambda}^y = \mathbf{1}_{\mu}^y$, and otherwise set $c_k(\lambda) = 0$. Define the set of *finite dots* to be

$$F^y(\lambda) = \{f = (f_1, \dots, f_n) \in \{0, 1\}^n \mid 0 \leq f_k \leq c_k(\lambda)\}.$$

The set of *sandwiched dots* is $S^y(\lambda) = A^y(\lambda) \cup F^y(\lambda)$. Note that $a_k \neq 0$ can only happen for affine coordinates $\mathbf{x}_{\kappa}(\lambda)_k > \mathbf{x}_{\kappa}(f)$.

Example 5D.3. We continue with Example 5C.17.

The condition $\mathbf{x}_{\kappa}(\lambda)_k \leq \mathbf{x}_{\kappa}(f)$ implies that $A^y(\lambda_1) = A^y(\lambda_2) = A^y(\lambda_3) = \{(0, 0, 0)\}$. Moreover, all strings associated to the second and third component have affine coordinates so $A^y(\mu_1) = \{(0, 0, n) \mid n \in \mathbb{Z}_{\geq 0}\}$ and $A^y(\mu_2) = \{(0, m, n) \mid m, n \in \mathbb{Z}_{\geq 0}\}$.

For the finite dots we have $F^y(\lambda_1) = F^y(\lambda_3) = \{(0, 0, 0), (0, 0, 1)\}$ and $F^y(\lambda_2) = F^y(\mu_1) = F^y(\mu_2) = \{(0, 0, 0)\}$. We also have $F^y(\lambda_1) = \{(0, 0, 0), (0, 0, 1)\}$ for type $D_{3+1}^{(2)}$. \diamond

5E. **Permutation diagrams.** We need the same tableaux as in AC types:

Definition 5E.1. Let $\mathbf{x}_{\underline{\kappa}}^A(-)$ denote the type A positioning function, see [MT21, Definition 6A.4]. Let $\lambda, \mu \in \underline{P}_{\ell, n}^{\rho, all}$. A λ -tableau of type μ is a bijection $T: \lambda \rightarrow \mathbf{x}_{\underline{\kappa}}^A(\mu)$. Such a tableau is *semistandard* if:

- (a) $T(m, 1, 1) \leq \kappa_m$ for $1 \leq m \leq \ell$.
- (b) $T(m, r, c) + 1 < T(m, r - 1, c)$ for all $(m, r, c), (m, r - 1, c) \in \lambda$.
- (c) $T(m, r, c) < T(m, r, c - 1) + 1$ for all $(m, r, c), (m, r, c - 1) \in \lambda$.

Let $\text{SStd}_{\hat{\kappa}}(\lambda, \mu)$ be the set of semistandard λ -tableaux of type μ and set $\text{SStd}_{\hat{\kappa}}(\lambda) = \bigcup_{\mu} \text{SStd}_{\hat{\kappa}}(\lambda, \mu)$.

Definition 5E.2. For $T \in \text{SStd}_{\hat{\kappa}}(\lambda, \mu)$ define the permutation $w_T \in \mathfrak{S}_n$ by requiring that

$$x_{w_T(k)}^{\mu} = T(m, r, c) \text{ whenever } x_k^{\lambda} = \mathbf{x}_{\underline{\kappa}}^A(m, r, c), \text{ for } 1 \leq k \leq n \text{ and } (m, r, c) \in \lambda.$$

This defines the *permutation diagram* $D_T = D(w_T)$ from $\mathbf{x}_{\underline{\kappa}}(\mu)$ to $\mathbf{x}_{\underline{\kappa}}(\lambda)$, as in Notation 3C.2.

In other words, a semistandard λ -tableau T of type μ is a filling of the nodes of λ with the type A coordinates of μ together with an anchor condition and such that the fillings decrease along rows and columns with an offset of 1. The associated permutation has top points defined by $\mathbf{x}_{\underline{\kappa}}(\lambda)$, bottom points by $\mathbf{x}_{\underline{\kappa}}(\mu)$ and permutes them according to the entries of T .

Example 5E.3. For $e = 2$ let $n = 6$, $\ell = 1$, $\kappa = (0)$ and $\varepsilon = 0.05$. Fix $\lambda = (5, 1)$ and $\mu = (3, 2, 1)$ for $\rho = (2)$. Then $\mathbf{x}_{\underline{\kappa}}^A(\lambda) = (-0.15, -0.05, 0.9, 1.85, 2.8, 3.75)$ and $\mathbf{x}_{\underline{\kappa}}^A(\mu) = (-0.25, -0.15, -0.05, 0.8, 0.9, 1.85)$. Two semistandard λ -tableaux, one of type λ one of type μ , are:

$$S = \begin{array}{|c|c|c|c|c|} \hline -0.05 & 0.9 & 1.85 & 2.8 & 3.75 \\ \hline & -0.15 & & & \\ \hline \end{array}, \quad D_S = 1_{\lambda}, \quad T = \begin{array}{|c|c|c|c|c|} \hline -0.15 & 0.8 & -0.05 & 0.9 & 1.85 \\ \hline & -0.25 & & & \\ \hline \end{array} \rightsquigarrow \begin{array}{c} | \quad | \quad | \quad | \\ | \quad | \quad | \quad | \\ | \quad | \quad | \quad | \\ | \quad | \quad | \quad | \end{array} \begin{array}{c} \nearrow \quad \searrow \\ \nearrow \quad \searrow \\ \nearrow \quad \searrow \\ \nearrow \quad \searrow \end{array} \begin{array}{c} | \quad | \\ | \quad | \\ | \quad | \\ | \quad | \end{array} \begin{array}{c} \uparrow \\ \uparrow \\ \uparrow \\ \uparrow \end{array} \begin{array}{c} \mathbf{x}_{\underline{\kappa}}^A(\lambda) \\ \text{read} \\ \mathbf{x}_{\underline{\kappa}}^A(\mu) \end{array}.$$

The tableau S is the *canonical λ -tableau* where all nodes are filled with their coordinates. Its associated permutation diagram is the identity. The permutation diagram D_T is build from the permutation illustrated above, which connects $\mathbf{x}_{\underline{\kappa}}^A(\mu)$ to $\mathbf{x}_{\underline{\kappa}}^A(\lambda)$, using $\mathbf{x}_{\underline{\kappa}}(\mu)$ at the bottom and $\mathbf{x}_{\underline{\kappa}}(\lambda)$ at the top. \diamond

5F. **Basis diagrams.** We consider the following set of endpoints X .

Definition 5F.1. Let $\underline{P}_{\ell, 0}^{\rho} = \{(\emptyset | \dots | \emptyset)\}$. For $n \geq 1$ let $\underline{P}_{\ell, n}^{\rho} \subseteq \underline{P}_{\ell, n}^{\rho, all}$ be the set defined by the condition that $\lambda \in \underline{P}_{\ell, n}^{\rho}$ only if $\lambda = \mu \cup \alpha$, where $\mu \in \underline{P}_{\ell, n-1}^{\rho}$ and α is an addable i -node of μ such that:

$$\text{whenever } \beta \text{ is an addable } i\text{-node of } \mu \text{ with } \mathbf{x}_{\underline{\kappa}}(\beta) < \mathbf{x}_{\underline{\kappa}}(\alpha), \text{ then } \mathbf{x}_{\underline{\kappa}}(\beta) \leq \mathbf{x}_{\underline{\kappa}}(\alpha).$$

Finally, let X be the set of all coordinates $\mathbf{x}_{\underline{\kappa}}(\lambda)$ for all $\lambda \in \underline{P}_{\ell, n}^{\rho}$.

Remark 5F.2. In general, only a handful of the elements of $\underline{P}_{\ell, n}^{\rho, all}$ belong to $\underline{P}_{\ell, n}^{\rho}$ as the rule in Definition 5F.1 allows only the addition of affine nodes as far to the left as possible.

We are ready for our main definition:

Definition 5F.3. For $\lambda \in \underline{P}_{\ell, n}^{\rho}$ set

$$(5F.4) \quad D_{ST}^{a, f} = (D_S)^* S_{\lambda}^{a, f} D_T = (D_S)^* y^a y^f \mathbf{1}_{\lambda}^y D_T$$

for $\mathbf{a} = (a_1, \dots, a_n) \in \mathbb{Z}_{\geq 0}^n$, $\mathbf{f} = (f_1, \dots, f_n) \in \{0, 1\}^n$, $S \in \text{SStd}_{\hat{\kappa}}(\lambda, \nu)$, $T \in \text{SStd}_{\hat{\kappa}}(\lambda, \mu)$.

We call $S_{\lambda}^{a, f} = y^a y^f \mathbf{1}_{\lambda}^y$ the *sandwiched part*, y^a the *affine part*, and y^f the *finite part* of $D_{ST}^{a, f}$. The following are the bases that we consider:

Definition 5F.5. Let $D_{ST}^f = D_{ST}^{(0, \dots, 0), f}$. We define

$$(5F.6) \quad \mathcal{B}_{\mathcal{W}_n^{\rho}(X)} = \{D_{ST}^{a, f} \mid \lambda \in \underline{P}_{\ell, n}^{\rho}, S, T \in \text{SStd}_{\hat{\kappa}}(\lambda), \mathbf{a} \in A^y(\lambda), \mathbf{f} \in F^y(\lambda)\}.$$

$$(5F.7) \quad \mathcal{B}_{\mathcal{B}_n^{\rho}(X)} = \{D_{ST}^f \mid \lambda \in \underline{P}_{\ell, n}^{\rho}, S, T \in \text{SStd}_{\hat{\kappa}}(\lambda), \mathbf{f} \in F^y(\lambda)\}.$$

Remark 5F.8. Note that we use $D_{ST}^{a, f}$ in (5F.4) below to distinguish it from the abstract definition. Of course, these elements are the C_{ST}^b in Definition 2A.2.

Remark 5F.9. The relevant picture for (5F.6) is:

$$D_{ST}^{a,f} \rightsquigarrow \begin{array}{c} \text{S} \\ \text{S}_\lambda^{a,f} \\ \text{T} \end{array} = \begin{array}{c} \text{S} \\ y^a \\ y^f \\ \mathbf{1}_\lambda^y \\ \text{T} \end{array}, \quad \begin{array}{l} \text{S} \text{ a permutation diagram,} \\ y^a \text{ a dot placement (the affine part),} \\ y^f \text{ a dot placement (the finite part),} \\ \mathbf{1}_\lambda^y \text{ a dotted idempotent,} \\ \text{T a permutation diagram.} \end{array}$$

This is the same as in AC types, which one crucial difference: in AC types the finite part is trivial.

5G. Homogeneous (affine) sandwich cellular bases. The order is as in [MT21, Definition 7C.1]:

Definition 5G.1. Let $\lambda, \mu \in \underline{P}_{\ell,n}^\rho$. Then λ *dominates* μ , written $\lambda \triangleright \mu$, if there exists a bijection $d: \lambda \rightarrow \mu$ such that $\mathbf{x}_{\kappa}(\alpha) \geq \mathbf{x}_{\kappa}(d(\alpha))$ and the solid string in $\mathbf{1}_\lambda$ at position $\mathbf{x}_{\kappa}(\alpha)$ has at least as many dots as the solid string in $\mathbf{1}_\mu$ at position $\mathbf{x}_{\kappa}(d(\alpha))$, for all $\alpha \in \lambda$. Write $\lambda \triangleright \mu$ if $\lambda \triangleright \mu$ and $\lambda \neq \mu$.

We are now ready to define (involutive) bases for $\mathscr{W}_n^\rho(X)$ and $\mathscr{R}_n^\rho(X)$. Recall that we are working with BAD types. We also use the Q -polynomials as in (3A.1).

The cell datum $\mathscr{C} = (\underline{P}_{\ell,n}^\rho, T, S, B_{\mathscr{W}_n^\rho(X)}, \deg, (-)^*)$ that we use is:

- The middle is $\underline{P}_{\ell,n}^\rho = (\underline{P}_{\ell,n}^\rho, \triangleright)$,
- $T = \bigcup_{\lambda \in \underline{P}_{\ell,n}^\rho} \text{SStd}_\kappa$ is the bottom/top set,
- the sandwiched part is $S_\lambda = R\{S_\lambda^{a,f} \mid \mathbf{a} \in A^y(\lambda), \mathbf{f} \in F^y(\lambda)\}$ for $\lambda \in \underline{P}_{\ell,n}^\rho$,
- we take $B_{\mathscr{W}_n^\rho(X)}$ from (5F.6), viewed as a map, as our basis,
- the degree is $S \mapsto \deg D_S$,
- the antiinvolution is the diagrammatic antiinvolution $(-)^*$.

The proof of the following theorem is postponed to Section 6 below.

Theorem 5G.2. *The datum \mathscr{C} is a graded affine sandwich cell datum for $\mathscr{W}_n^\rho(X)$. In particular, (5F.6) is a homogeneous affine sandwich cellular basis for $\mathscr{W}_n^\rho(X)$.*

If we replace $S_\lambda = R\{S_\lambda^{a,f} \mid \mathbf{a} \in A^y(\lambda), \mathbf{f} \in F^y(\lambda)\}$ with $S_\lambda^c = R\{S_\lambda^{(0,\dots,0),f} \mid \mathbf{f} \in F^y(\lambda)\}$, and $B_{\mathscr{W}_n^\rho(X)}$ with $B_{\mathscr{R}_n^\rho(X)}$, then Theorem 5G.2 and comparing the definitions directly implies:

Corollary 5G.3. *The datum $\mathscr{C} = (\underline{P}_{\ell,n}^\rho, T, S^c, B_{\mathscr{R}_n^\rho(X)}, \deg, (-)^*)$ is a graded affine sandwich cell datum for $\mathscr{R}_n^\rho(X)$. In particular, (5F.7) is a homogeneous sandwich cellular basis for $\mathscr{R}_n^\rho(X)$. \square*

Define a semistandard tableaux $S \in \text{SStd}_\kappa(\lambda)$ to be *standard* if it is of type $\omega = (n|0|\dots|0)$. Let $\text{Std}(\lambda)$ be the set of standard λ -tableaux. Let $\mathscr{W}_n^\rho = \mathbf{1}_\omega \mathscr{W}_n^\rho(X) \mathbf{1}_\omega$ and $\mathscr{R}_n^\rho = \mathbf{1}_\omega \mathscr{R}_n^\rho(X) \mathbf{1}_\omega$ be the associated KLR and cyclotomic KLR algebra, respectively. This terminology is justified at the end of Section 3C. We use E instead of D to refer to the basis elements of the idempotent truncations. We will not highlight the cell datum below.

Proposition 5G.4. *The set $B_{\mathscr{W}_n^\rho} = \{E_{st}^{a,f} \mid \lambda \in \underline{P}_{\ell,n}^\rho, S, T \in \text{Std}(\lambda), \mathbf{a} \in A^y(\lambda), \mathbf{f} \in F^y(\lambda)\}$ is a homogeneous affine sandwich cellular basis of \mathscr{W}_n^ρ .*

Proof. Apply [MT21, Proposition 3F.1 and Example 6A.11]. \square

As before we obtain:

Corollary 5G.5. *The set $B_{\mathscr{R}_n^\rho} = \{E_{st}^f \mid \lambda \in \underline{P}_{\ell,n}^\rho, S, T \in \text{Std}(\lambda), \mathbf{f} \in F^y(\lambda)\}$ is a homogeneous sandwich cellular basis of \mathscr{R}_n^ρ . \square*

Let us now discuss the upshot of Theorem 5G.2 and Corollary 5G.3 for simple modules. To this end, let $a(\lambda)$ and $f(\lambda)$ be the number of possible non-zero positions of $A^y(\lambda)$ and $F^y(\lambda)$, respectively.

Lemma 5G.6. *For all $\lambda \in \underline{P}_{\ell,n}^\rho$ we have $S_\lambda \cong R[X_1, \dots, X_{a(\lambda)}] \otimes R[Y_1, \dots, Y_{f(\lambda)}] / (Y_i^2 = 0)$ and $S_\lambda^c \cong R[Y_1, \dots, Y_{f(\lambda)}] / (Y_i^2 = 0)$.*

Proof. The first claim, regarding the X_i , follows by using Proposition 3D.1. For the second claim, regarding the Y_i , we inductively pull strings and jump dots to the right. That is, if one of the strings corresponding to possible non-zero positions of $F^y(\lambda)$ carries two dots we can use (4A.5) and the claim follows inductively. \square

Proposition 5G.7. *The algebra $\mathscr{R}_n^\rho(X)$ is free of rank $\sum_{\lambda \in \underline{P}_{\ell,n}^\rho} 2^{f(\lambda)} (\#\text{SStd}_\kappa)^2$, and $\mathscr{W}_n^\rho(X)$ is free of rank $\sum_{\lambda \in \underline{P}_{\ell,n}^\rho} 2^{f(\lambda)} (\#\text{Std})^2$.*

Proof. Directly from [Lemma 5G.6](#) and the respective corollaries above. \square

By the above, it is also easy to write down the graded dimensions of these algebras.

Remark 5G.8. [Proposition 5G.7](#) generalizes the dimension formulas from [[AP14](#), Corollary 3.5] and [[AP16](#), Corollary 3.3].

Example 5G.9. It is illustrative to compare the combinatorics for types $C_2^{(1)}$, $A_{2,2}^{(2)}$ and $D_{2+1}^{(2)}$. (See [[MT21](#), Section 7] for the relevant constructions in type $C_e^{(1)}$.) We will ignore the affine part in this example. Fix $\ell = 1$, $\kappa = (0)$ and $\rho = (0)$ and take $\beta = (0, 1, 2) \in I^3$. We are first looking for all 1-partitions of 3 that have β as their *residue sequence*, that is, $\lambda \in \mathbb{P}_{\ell,4}^\rho$ whose nodes have residues β in row reading order. We get the following 1-partitions:

$$C_2^{(1)}, A_{2,2}^{(2)}, D_{2+1}^{(2)} : \lambda_1 = \begin{array}{|c|c|c|} \hline 0 & 1 & 2 \\ \hline \end{array}, \quad C_2^{(1)}, A_{2,2}^{(2)} : \lambda_3 = \begin{array}{|c|} \hline 0 \\ \hline 1 \\ \hline 2 \\ \hline \end{array}.$$

The dotted idempotents for types $A_{2,2}^{(2)}$ and $D_{2+1}^{(2)}$ are displayed in [Example 5C.17](#), and the ones for type $C_2^{(1)}$ have the same form as the ones for type $A_{2,2}^{(2)}$. The sets of finite dots for types $A_{2,2}^{(2)}$ and $D_{2+1}^{(2)}$ are listed in [Example 5D.3](#), while the set of finite dots is always trivial in type $C_2^{(1)}$. Thus, we get by using [Theorem 5G.2](#) that

$$\begin{array}{c|c|c|c|} \beta = (0, 1, 2) & C_2^{(1)} & A_{2,2}^{(2)} & D_{2+1}^{(2)} \\ \hline \# \text{ tableaux} & 2 & 2 & 1 \\ \hline \text{graded dim} & 1 + q^2 & (1 + q^2)(1 + q^4) & 1 + q^2 \end{array}, \quad \begin{array}{c|c|c|c|} \beta' = (2, 1, 0) & C_2^{(1)} & A_{2,2}^{(2)} & D_{2+1}^{(2)} \\ \hline \# \text{ tableaux} & 2 & 1 & 1 \\ \hline \text{graded dim} & 1 + q^2 & 1 & 1 + q^2 \end{array}.$$

Here we have listed the graded dimension (using the usual q -notation indicating the degree) of the idempotent truncation of $\mathcal{R}_\beta^\rho(X)$ determined by β . We also listed the relevant numbers for $\beta' = (2, 1, 0)$ where $\rho = (2)$. These numbers match [[HS21](#), Theorem 1.1], which is expected as this case is the cyclotomic KLR algebra of the respective types. \diamond

Proposition 5G.10. *Suppose that R is a field, and let $(\underline{\mathbb{P}}_{\ell,n}^\rho)^{\neq 0}$ or $(\mathbb{P}_{\ell,n}^\rho)^{\neq 0}$ denote the sets of apexes.*

- (a) *For a fixed apex $\lambda \in (\underline{\mathbb{P}}_{\ell,n}^\rho)^{\neq 0}$ there exist a 1:1-correspondence between simple $\mathcal{W}_n^\rho(X)$ -modules with apex λ and $R^{\alpha(\lambda)}$. Moreover, up to isomorphism, there exists exactly one graded simple $\mathcal{W}_n^\rho(X)$ -module of that apex.*
- (b) *For a fixed apex $\lambda \in (\mathbb{P}_{\ell,n}^\rho)^{\neq 0}$ there exists exactly one simple, and one graded simple, $\mathcal{R}_n^\rho(X)$ -module of that apex up to isomorphism.*

Proof. This is a combination of [Theorem 2A.4](#) and the results from this section. For example, the explicit parametrization of the simple modules for fixed apexes follows from [Lemma 5G.6](#). \square

6. PROOF OF CELLULARITY

We are now ready to prove [Theorem 5G.2](#).

Remark 6A.1. As before, the combinatorics below is separated into usual and shifted partition combinatorics. The former is very similar to type $C_e^{(1)}$, which was covered in [[MT21](#), Section 7], so we focus on the shifted partition combinatorics.

As in [[MT21](#), Section 7E] the most important notion that we need is that of Young equivalence. To define it we need some preliminary notions.

Definition 6A.2. For $i, j \in I$, a *close (i, i, i) -triple*, respectively a *close (i, j, k) -triple* or a *close (i, j, j, i) -quadruple*, is a collection of close strings as in the following local configurations:

$$(6A.3) \quad \text{triple: } \begin{array}{|c|} \hline i \\ \hline i \\ \hline i \\ \hline \end{array}, \quad \text{triple: } \left(\begin{array}{|c|} \hline i \\ \hline k \\ \hline \vdots \\ \hline j \\ \hline \end{array} \text{ or } \begin{array}{|c|} \hline j \\ \hline \vdots \\ \hline i \\ \hline k \\ \hline \end{array} \right) \quad \text{and} \quad \left(\text{quadruple: } \begin{array}{|c|} \hline i \\ \hline i \\ \hline \vdots \\ \hline j \\ \hline j \\ \hline \end{array} \text{ or } \begin{array}{|c|} \hline j \\ \hline j \\ \hline \vdots \\ \hline i \\ \hline i \\ \hline \end{array} \right).$$

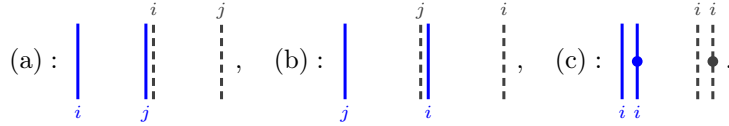
We also need the following, which should be compared with [Remark 5C.7](#). Here we consider the two ghost 1-strings in type $D_{e+1}^{(2)}$ as one string.

Definition 6A.4. Let S be a dotted straight line diagram. Solid i and j -strings of S are *pseudo row equivalent* if either:

- (a) $i \rightsquigarrow j$, there are no dots on the i or j -strings, and the ghost i -string is close and to the left of the solid j -string;
- (b) $i \leftarrow j$, there are no dots on the i or j -strings, and the solid i -string is close and to the left of the ghost j -string;
- (c) $i = j$ is a multisink, the i -string carries a dot, and the solid i -string is close and to the right of the solid j -string;

A pseudo row equivalence class is a **row equivalence class** if there are no close (i, i, i) -triples, the only close (i, j, k) -triples are of the form $(i, i + 1, i + 2)$ or $(i, i - 1, i - 2)$, or $(1, 0, 1)$ in type $A_{2,e}^{(2)}$, and if (i, j, j, i) is a close quadruple, then j is a multisink and either $i \rightsquigarrow j$ or $i \leftarrow j$.

The illustrations for parts (a)–(c) of [Definition 6A.4](#) are:



These should be compared with [\(5C.8\)](#) and [\(5C.10\)](#). Note that [\(5C.9\)](#) is also included in the description since pseudo row equivalence classes only take two strings per step into account.

Definition 6A.5. Assume that we are in the case of shifted partitions. A **Young equivalence class** Y of solid strings in S is a disjoint union of row equivalence classes $R_1 \cup \dots \cup R_z$ such that:

- (a) The first string in R_1 has no dot and is close to an (affine) red string of the same residue;
- (b) $|R_1| > |R_2| > \dots > |R_z|$;
- (c) the first string in R_{a+1} is an i -string, and close to a dotted solid i -string of the same residue in R_a or there is a j -string in R_a that satisfies one of closeness conditions in (a) and (b) of [Definition 6A.4](#) with respect to this string.

For usual partitions we use the analog of [\[MT21, Definition 7E.6\]](#). That is, (b) above is replaced with $|R_1| \geq |R_2| \geq \dots \geq |R_z|$ and (c) mimics [\(5C.11\)](#) with a dot on the i -string in the first two cases therein.

Recall that $L(S)$ is the left-justification of the dotted straight line diagram S as e.g. in [Example 3C.5](#).

Lemma 6A.6. Let S be a dotted straight line diagram. Then $L(S) = L(\mathbf{1}_\lambda^y)$, for some $\lambda \in \underline{\mathbb{P}}_{\ell,n}^p$, if and only if the solid strings of S are a disjoint union of Young equivalence classes.

Proof. By construction, the solid strings in $\mathbf{1}_\lambda^y$ are a disjoint union of Young equivalence classes cf. [Remark 5C.7](#).

To prove the converse, given a dotted straight line diagram S , we construct an ℓ -partition λ by inductively associating the solid strings in each Young equivalence class Y to nodes of a component $\lambda^{(m)}$ of λ . We explain the situation of shifted partitions, that is, when ρ_m is a multisink. The case of usual partitions can be proven similarly, following [\[MT21, Lemma 7E.8\]](#).

By [Definition 6A.5\(a\)](#), the first string of Y is left adjacent to an (affine) red string of the same residue. If this is the m th red string, then identify the solid string with the node $(m, 1, 1)$. By induction we now assume that the k th solid i -string in Y corresponds to the node $(m, r, c) \in \lambda$. There are two cases to consider.

Case 1. First, if i is not the last string in its row equivalence class, then [\(5C.8\)](#), [\(5C.9\)](#) and [\(5C.10\)](#) correspond to (a)–(c) of [Definition 6A.4](#) and the condition on close (i, j, k) -triples and close (j, i, i, j) -quadruples, with the correct dot placement. Moreover, no other configurations can appear, i.e. there are no close (i, i, i) -triples or any other triples or quadruples due to (a)–(c) of [Definition 6A.4](#). Hence, the $(k+1)$ st solid j -string corresponds to the node $(m, r, c+1)$.

Case 2. If on the other hand i is the last string in its row equivalence class, then we observe that [\(5C.11\)](#) corresponds to [Definition 6A.5\(c\)](#), and the $(k+1)$ st solid j -string corresponds to the node $(m, r+1, c)$.

Finally, note that the condition in [Definition 6A.5\(b\)](#) ensures that the result is a shifted ℓ -partition. \square

Proposition 6A.7. Suppose that $D \in \mathcal{W}_n^p(X)$ and that D factors through the dotted idempotent diagram S . Then there exists $\lambda \in \underline{\mathbb{P}}_{\ell,n}^p$ such that D factors through $\mathbf{1}_\lambda^y$ and $\lambda \triangleright L(S)$.

Proof. Without loss of generality we can assume that $D = S$. If $D = \mathbf{1}_\lambda^y$, then there is nothing to prove by [Lemma 6A.6](#). So assume that [Lemma 6A.6](#) is not satisfied, i.e. that D is not a disjoint union of Young equivalence classes.

We can assume that all strings are within $[\min X, \max X + 1] \times [0, 1]$, the **region defined by X** . Let s be the rightmost solid string in D that is not in any Young equivalence class. We want to argue that we can pull s to the right, jump dots on s further to the right, or we can attach s to a Young equivalence class, which implies the claim by induction. There are a few cases which we need to discuss. We only consider

shifted partition combinatorics since the arguments for usual partition combinatorics are mutatis mutandis as in [MT21, Proposition 7E.9].

Case 1a. s is the rightmost string in the sense that we can pull it arbitrarily far to the right, and s does not have a dot. In this case we can park it next to an affine red string of the same residue, and it is now part of a Young equivalence class by Definition 6A.5.(a).

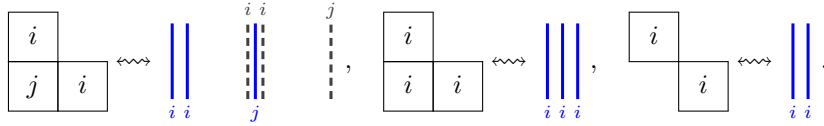
Case 1b. As in Case 1a, but now s carries a dot. After pulling the dot to the top of the diagram, the same argument as in Case 1a works.

We will now assume that we are not in Cases 1a and 1b. Then, up to isotopy, s or its ghost is close and to the right of a solid, ghost or red string t . We focus on the situation when s is close to t , where we again have several cases. The cases where the ghost of s is close to t follow mutatis mutandis and are omitted. We also assume that s does not carry a dot. If it does, then there is an additional extra argument one needs to make as explained in [MT21, Proof of Proposition 7E.9, Case 5] (this argument works mutatis mutandis in the BAD types), but in the end the relation used below allow us to continue with the induction.

Case 2a. Assume that s is not in the Young equivalence class of t because the close (i, j, k) -triple condition is not satisfied for s being the leftmost string in (6A.3). In this case the right-hand relation in (4A.4) applies. (This works unless we in a close $(1, 0, 1)$ -triple situation in type $A_{2,e}^{(2)}$, where we do not want to pull s further.)

Case 2b. Similarly, assume that s is not in the Young equivalence class of t because the close (i, j, j, i) -quadruple condition is not satisfied for s being the leftmost string in (6A.3). Then we can use Lemma 4A.6 to pull s further to the right.

Case 2c. We now assume that s is not in the Young equivalence class of t because the condition $|R_1| > |R_2| > \dots > |R_z|$ is not satisfied. For $i, j \in I$ and $i \rightsquigarrow j$ or $i \leftarrow j$, the crucial configurations are



There are a few cases, but for all these we can use (4A.3) or (4A.4) to pull s to the right.

Assume now that we are not in any of the cases above.

Case 3a. If t is an (affine) red string, then a Reidemeister II move pulls s further to the right. We can apply such a move since the case where s has the same residue as t is covered above.

Case 3b. If t is a solid string, then a Reidemeister II applies unless s has the same residue as t . In this latter case (4A.3) applies.

Case 3c. Finally, if t is a ghost string, then we can use a Reidemeister II relation to pull s rightwards. To see this note that the assumption that s and t are not in a Young equivalence class imply that s and t are not as in (a) and (b) of Definition 6A.4, or as in Definition 6A.5.(c).

Hence, the result follows by induction. \square

The rest of the proof of Theorem 5G.2 is essentially the same as in [MT21, Section 7E]. That is, applying dots or crossings to $\mathbf{1}_\lambda^y$ gives a linear combination of bigger elements. To this end, recall the definition of the finite dots from Definition 5D.2.

Lemma 6A.8. *Suppose that $\lambda \in P_{\ell,n}^\rho$ and $1 \leq m \leq n$. Then $y_m y_m^{c_m(\lambda)} \mathbf{1}_\lambda^y \in \mathscr{W}_n^{\triangleright \lambda}$.*

Proof. We can use Proposition 6A.7 so that $y_m y_m^{c_m(\lambda)} \mathbf{1}_\lambda^y$ factors through $\mathbf{1}_\mu^y$ for $\mu \triangleright \lambda$. \square

Consider λ as a composition, and let \mathfrak{S}_λ be the associated Young subgroup of \mathfrak{S}_n .

Lemma 6A.9. *Suppose that $\lambda \in P_{\ell,n}^\rho$ and $w \in \mathfrak{S}_\lambda$. Then $D_\lambda(w) \mathbf{1}_\lambda, \mathbf{1}_\lambda D_\lambda(w) \in \mathscr{W}_n^{\triangleright \lambda}$.*

Proof. As in [MT21, Lemma 6D.17]. \square

Proof of Theorem 5G.2. The arguments given in [MT21, Sections 6D and 7E], which are the analogous statements for the AC types, apply in BAD types as well. In fact, these arguments are general and use only Proposition 3D.1 and Remark 3D.2, as well as the analogs of the results proven above. \square

Remark 6A.10. If one agrees with the strategy in Remark 4A.1, then the construction of the homogeneous (affine) sandwich cellular basis and proof of Theorem 5G.2 splits into several parts:

- (a) Because the bottom and top will be given by permutation diagrams, the first step is to find tableaux combinatorics associated to the quiver under study. For a general quiver this is potentially hopeless, but for a lot of quivers an answer is already in the literature.
- (b) The construction of the middle is then crucial. This part is noncanonical, although mostly dictated by Remark 4A.1 and we hope to explain a more general approach in future work. Note that additional dots might be necessary to prevent basis elements being annihilated by (3A.3) and to have the analog of Lemma 5C.18.

- (c) From here onwards the arguments are general and do not depend on the quiver anymore: [Proposition 6A.7](#) follows by analyzing the combinatorics of the string placement of $\mathbf{1}_\lambda$, and this proposition in turn directly implies [Lemma 6A.8](#) and [Lemma 6A.9](#). Once these two lemmas have been established the proof of cellularity [Theorem 5G.2](#) is formal. Linear independence follows using the faithful polynomial module in [Remark 3D.2](#), spanning using [Lemma 6A.8](#) and [Lemma 6A.9](#) and the standard basis in [Proposition 3D.1](#). The latter arguments are independent of the underlying quiver.

REFERENCES

- [AST18] H.H. Andersen, C. Stroppel, and D. Tubbenhauer. Cellular structures using U_q -tilting modules. *Pacific J. Math.*, 292(1):21–59, 2018. URL: <https://arxiv.org/abs/1503.00224>, doi:10.2140/pjm.2018.292.21.
- [AP14] S. Ariki and E. Park. Representation type of finite quiver Hecke algebras of type $A_{2\ell}^{(2)}$. *J. Algebra*, 397:457–488, 2014. URL: <https://arxiv.org/abs/1208.0889>, doi:10.1016/j.jalgebra.2013.09.005.
- [AP16] S. Ariki and E. Park. Representation type of finite quiver Hecke algebras of type $D_{\ell+1}^{(2)}$. *Trans. Amer. Math. Soc.*, 368(5):3211–3242, 2016. URL: <https://arxiv.org/abs/1305.6367>, doi:10.1090/tran/6411.
- [Bow17] C. Bowman. The many graded cellular bases of Hecke algebras. 2017. To appear in *Amer. J. Math.* URL: <https://arxiv.org/abs/1702.06579>.
- [ET21] M. Ehrig and D. Tubbenhauer. Relative cellular algebras. *Transform. Groups*, 26(1):229–277, 2021. URL: <https://arxiv.org/abs/1710.02851>, doi:10.1007/S00031-019-09544-5.
- [GL96] J.J. Graham and G. Lehrer. Cellular algebras. *Invent. Math.*, 123(1):1–34, 1996. doi:10.1007/BF01232365.
- [GMS09] O. Ganyushkin, V. Mazorchuk, and B. Steinberg. On the irreducible representations of a finite semigroup. *Proc. Amer. Math. Soc.*, 137(11):3585–3592, 2009. URL: <https://arxiv.org/abs/0712.2076>, doi:10.1090/S0002-9939-09-09857-8.
- [Gre51] J.A. Green. On the structure of semigroups. *Ann. of Math. (2)*, 54:163–172, 1951. doi:10.2307/1969317.
- [GW15] N. Guay and S. Wilcox. Almost cellular algebras. *J. Pure Appl. Algebra*, 219(9):4105–4116, 2015. doi:10.1016/j.jpaa.2015.02.010.
- [HM10] J. Hu and A. Mathas. Graded cellular bases for the cyclotomic Khovanov–Lauda–Rouquier algebras of type A . *Adv. Math.*, 225(2):598–642, 2010. URL: <http://arxiv.org/abs/0907.2985>, doi:10.1016/j.aim.2010.03.002.
- [HS21] J. Hu and L. Shi. Graded dimensions and monomial bases for the cyclotomic quiver Hecke algebras. 2021. URL: <https://arxiv.org/abs/2108.05508>.
- [Kac90] V.G. Kac. *Infinite-dimensional Lie algebras*. Cambridge University Press, Cambridge, third edition, 1990. doi:10.1017/CB09780511626234.
- [KL09] M. Khovanov and A.D. Lauda. A diagrammatic approach to categorification of quantum groups. I. *Represent. Theory*, 13:309–347, 2009. URL: <https://arxiv.org/abs/0803.4121>, doi:10.1090/S1088-4165-09-00346-X.
- [KL11] M. Khovanov and A.D. Lauda. A diagrammatic approach to categorification of quantum groups II. *Trans. Amer. Math. Soc.*, 363(5):2685–2700, 2011. URL: <https://arxiv.org/abs/0804.2080>, doi:10.1090/S0002-9947-2010-05210-9.
- [KL15] A.S. Kleshchev and J.W. Loubert. Affine cellularity of Khovanov–Lauda–Rouquier algebras of finite types. *Int. Math. Res. Not. IMRN*, (14):5659–5709, 2015. URL: <https://arxiv.org/abs/1310.4467>, doi:10.1093/imrn/rnu096.
- [KX12] S. König and C. Xi. Affine cellular algebras. *Adv. Math.*, 229(1):139–182, 2012. doi:10.1016/j.aim.2011.08.010.
- [MT21] A. Mathas and D. Tubbenhauer. Subdivision and cellularity for weighted KLRW algebras. 2021. URL: <https://arxiv.org/abs/2111.12949>.
- [Rou08] R. Rouquier. 2-Kac–Moody algebras. 2008. URL: <http://arxiv.org/abs/0812.5023>.
- [Rou12] R. Rouquier. Quiver Hecke algebras and 2-Lie algebras. *Algebra Colloq.*, 19(2):359–410, 2012. URL: <https://arxiv.org/abs/1112.3619>, doi:10.1142/S1005386712000247.
- [TV21] D. Tubbenhauer and P. Vaz. Handlebody diagram algebras. 2021. URL: <https://arxiv.org/abs/2105.07049>.
- [Web17] B. Webster. Rouquier’s conjecture and diagrammatic algebra. *Forum Math. Sigma*, 5:e27, 71, 2017. URL: <https://arxiv.org/abs/1306.0074>, doi:10.1017/fms.2017.17.
- [Web19] B. Webster. Weighted Khovanov–Lauda–Rouquier algebras. *Doc. Math.*, 24:209–250, 2019. URL: <https://arxiv.org/abs/1209.2463>, doi:10.25537/dm.2019v24.209-250.

A.M.: THE UNIVERSITY OF SYDNEY, SCHOOL OF MATHEMATICS AND STATISTICS F07, OFFICE CARSLAW 718, NSW 2006, AUSTRALIA, WWW.MATHS.USYD.EDU.AU/U/MATHAS/
 Email address: andrew.mathas@sydney.edu.au

D.T.: THE UNIVERSITY OF SYDNEY, SCHOOL OF MATHEMATICS AND STATISTICS F07, OFFICE CARSLAW 827, NSW 2006, AUSTRALIA, WWW.DTUBBENHAUER.COM
 Email address: daniel.tubbenhauer@sydney.edu.au